Advancements in Photocured Graphene-Oxide Coatings: Enhancing Tribological Performance through Liquid Crystal Technologies

MINA FARID

A Thesis

in the department of

Mechanical, Industrial and Aerospace Engineering

Presented in Partial Fulfillment of the Requirements for the Degree of

Master of Applied Science (Mechanical Engineering)

at

Concordia University

Montréal, Québec, Canada

October, 2024

CONCORDIA UNIVERSITY
School of Graduate Studies

This is to certify that the thesis prepared

By: **Mina Farid**

Entitled: **Advancements in Photocured Graphene-Oxide Coatings: Enhancing Tribological Performance through Liquid Crystal Technologies**

and submitted in partial fulfillment of the requirements for the degree of

Master of Applied Science (Mechanical Engineering)

complies with the regulations of the University and meets the accepted standards with respect to originality and quality.

Signed by the final examining committee:

Prof. Martin D. Pugh Chair

Prof. Wael Saleh Examiner

Prof. Martin D. Pugh Examiner

Prof. Paula M Wood-Adams Thesis Supervisor

Prof. Pantcho P. Stoyanov Thesis C o - Supervisor

Approved by Prof. Sivakumar Narayanswamy
Graduate Program Director

October 2024

Prof. Mourad Debbabi

Dean of Gina Cody School of Engineering and Computer Science

Abstract

Advancements in Photocured Graphene-Oxide Coatings: Enhancing Tribological Performance through Liquid Crystal Technologies

Mina Farid

This thesis presents an exploration of advanced tribological coatings for improving wear resistance and reducing friction in mechanical components, particularly in industries like aerospace. Traditional coating methods such as physical vapor deposition and high-velocity oxygen fuel have limitations, necessitating innovative approaches. This research introduces the use of graphene oxide liquid crystals combined with photocuring to develop coatings that significantly enhance tribological performance. The liquid crystal self-assembly of graphene oxide in alcohol allows for dense ordering of platelets on substrates, and photocuring creates strong, covalent bonds between the platelets and the substrate, resulting in durable coatings.

Experimental results demonstrated a remarkable reduction of up to 72% in the friction coefficient compared to uncoated substrates. The study also explored the effects of annealing on coating performance, finding that annealed coatings exhibited lower friction and superior wear resistance for low graphene oxide contents. The research underscores the potential of photocured graphene oxide coatings to address the tribological challenges in critical applications, offering a cost-effective and environmentally sustainable solution that advances the field of coating materials science and engineering.

Acknowledgment

I would like to express my heartfelt gratitude to everyone who contributed to the successful completion of this thesis.

First and foremost, I extend my deepest appreciation to my supervisors, Dr. Paula Wood-Adams and Dr. Pantcho Stoyanov. Their invaluable guidance, expertise, and support have been instrumental throughout this research. Dr. Wood-Adams' insights and assistance in manuscript writing have greatly enhanced the quality of this work. Dr. Stoyanov's mentorship, advice, and unwavering support have been essential to the development and execution of this project.

I am also deeply grateful to the faculty and staff at Concordia University, particularly those in the laboratories where I conducted my research. The technical support, resources, and collaborative environment provided by the lab members have been crucial to the progress and success of this study.

My sincere thanks also go to the research teams associated with both of my supervisors. Their collaborative spirit and contributions have enriched my research experience and broadened my understanding of the field.

Finally, I would like to acknowledge the support of my family and friends for their encouragement and patience throughout this journey.

Thank you all for your contributions and support.

Contribution of Authors

This thesis is based on an under-review journal article. The manuscript has been produced with me as the principal author and Dr. Paula Wood-Adams and Dr. Pantcho Stoyanov as co-authors. The experimental work, technical analysis, and manuscript preparation have been carried out primarily by me, with substantial contributions from my co-authors. Below is a summary of the contributions:

Chapter 4: Farid, M, Wood-Adams, P., Stoyanov, P. (Photocured graphene-oxide liquid crystal coatings for improved tribological performance)

- Mina Farid was responsible for conceptualizing the project, designing and executing the experiments, and drafting the manuscript.
- Dr. Paula Wood-Adams assisted with data analysis and interpretation and contributed significantly to manuscript writing and provided valuable feedback and revisions.
- Dr. Pantcho Stoyanov provided guidance and support throughout the project, including data analysis and interpretation and critical review of the manuscript.

Table of Contents

List of Figures

List of Tables

Chapter 1. Introduction

1.1. Background

Wear and friction are critical factors impacting the performance and sustainability of mechanical components across various industries. In aerospace and other high-tech sectors, wear-related challenges have far-reaching economic and environmental consequences. Historical data reveal that wear-induced failures can be significantly costly, with potential economic savings of up to 95% achievable through innovative tribological solutions [1]. Friction and wear impact energy consumption, economic expenditure, and CO_2 emissions globally, affecting sectors such as transportation, manufacturing, and power generation [1]. Abrasive wear alone imposes costs equivalent to 1–4% of the gross national product of industrialized nations [2]. To address these challenges, there is a pressing need for effective wear mitigation strategies that minimize maintenance costs and environmental impact.

Traditional coating methods, including physical vapor deposition (PVD) and high-velocity oxygen fuel (HVOF) coatings, have limitations in terms of scalability and effectiveness under extreme conditions. Recent advancements have shifted focus towards alternative approaches, such as the use of ionic liquids and carbon nanotubes as lubricant additives [3]. These innovations offer more environmentally friendly lubrication solutions but still face challenges in achieving the desired wear resistance and performance improvements.

Graphene and graphene oxide (GO) coatings have emerged as promising alternatives due to their exceptional durability and tribological properties. However, scaling these coatings for practical applications has proven challenging. Graphene coatings, characterized by their high transmittance,

hydrophobicity, and strong adhesion, demonstrate improved tribological performance compared to conventional coatings [4], [5]. Recent studies, such as those by Shi et al. [24], highlight the potential of graphene-based copolymers for durable protective coatings, though their performance under extreme conditions remains under investigation.

Photopolymerization offers a method to modify material properties through light-induced chemical reactions, transitioning materials from liquid to solid or altering their solubility and adhesion characteristics [6]. This process, which includes free-radical or cationic photopolymerization, is employed in various applications such as printed circuit boards, photocurable coatings, and 3D printing [6], [7]. Challenges in photopolymerization involve controlling the specific wavelengths needed for effective reactions and mitigating UV degradation, which impacts the material's durability and environmental safety [7], [8].

Tribology is the study of friction, wear, lubrication, and their interrelationships. It is a multidisciplinary field that impacts various industries, including manufacturing, biomedical, automotive, and aerospace sectors. This literature review highlights recent advancements and key aspects of tribology, focusing on lubrication, wear mechanisms, surface engineering, biotribology, and computational tribology [9].

Lubrication plays a crucial role in reducing friction and wear in mechanical systems. Advances in lubrication technology have led to the development of high-performance lubricants that improve energy efficiency and reduce maintenance costs. Novel lubricants, such as ionic liquids and nanolubricants, have shown promise in enhancing lubrication under extreme conditions [10].

Understanding wear mechanisms is essential for predicting the lifespan of components and improving material performance. Recent research has focused on the microstructural changes that

occur during wear and the development of wear-resistant materials. High-entropy alloys and advanced ceramics are examples of materials with improved wear resistance [9].

Surface engineering techniques, such as coating and texturing, are employed to enhance the tribological properties of materials. These techniques aim to reduce friction and wear by modifying the surface characteristics. For instance, diamond-like carbon (DLC) coatings are widely used due to their low friction and high hardness [11]. While diamond-like carbon (DLC) coatings are widely used due to their low friction and high hardness, they also have several limitations that restrict their application in certain high-performance environments. DLC coatings often suffer from poor adhesion and high residual stresses, which can lead to delamination or cracking under high contact stresses, especially above 1 GPa [12]. Additionally, DLC coatings exhibit limited thermal stability, with performance degrading at elevated temperatures due to hydrogen depletion or oxidation processes, making them unsuitable for high-temperature applications like dry machining or hot forming [13]. These factors necessitate the exploration of alternative coatings for more demanding environments.

1.2. Rationale for the Study

This thesis aims to address the limitations of traditional wear mitigation methods and explore innovative solutions through the development of photocured graphene-oxide liquid crystal coatings. By leveraging advanced photopolymerization techniques and graphene oxide properties, the research seeks to enhance the performance, durability, and environmental sustainability of coatings used in high-demand applications such as aerospace.

Chapter 2. Literature Review

2.1. Current Tribological Challenges and Sustainability Concerns

2.1.1. Economic and Environmental Impact of Tribology in Industries

Neglecting wear in industries can lead to significant economic and environmental consequences. Studies show that wear-related failures were a major concern in the past, with potential economic savings of up to 95% achievable through new tribological solutions [1]. The impact of friction and wear on energy consumption, economic expenditure, and CO2 emissions is substantial globally, affecting sectors like transportation, manufacturing, power generation, and residential areas [1]. Abrasive wear alone costs industrialized nations 1–4% of their gross national product, emphasizing the need for effective wear mitigation strategies [2]. Implementing innovative solutions like utilizing ionic liquids and carbon nanotubes as lubricant additives can reduce friction losses and wear, offering a more environmentally friendly approach to industrial lubrication [3]. By focusing on developing new tribological solutions, utilizing advanced lubricants, and implementing surface coatings, industries can minimize maintenance costs and environmental impact associated with wear and tear phenomena [2].

2.1.2. Tribological Challenges in Aircraft Industry

Tribology, the study of friction, wear, and lubrication, plays a critical role in the safety and reliability of aircraft, particularly in the performance of gas turbine engines. The importance of tribological principles in aerospace engineering cannot be overstated, as they directly influence the lifespan of critical components, prevent system failures, and reduce maintenance costs. Studies

have shown that proper application of tribological systems in aircraft engines significantly impacts the longevity and reliability of these components, reducing the risk of wear-related failures [14]. Historical data from the aerospace industry has consistently shown that failures in tribological systems can lead to catastrophic accidents, underscoring the need for thorough understanding and application of tribological diagnostics and design improvements [15].

Wear damage on aircraft gas turbine blades can have significant effects on their performance and efficiency [16]. The presence of solid particles in the working fluid medium, such as sand, dust, and salts, can cause erosion damage, coating wear, and corrosion on the blade surfaces [17], [18]. This wear damage can lead to rapid performance deterioration, including loss of aircraft [19]. In addition, wear damage can result in changes to the blade geometry and aerodynamic properties, reducing the overall life of the compressor and the engine [20].

The operational reliability of aero-engines, especially gas turbines, is highly dependent on the wear and lubrication. Nidzgorska et al. (2023) emphasize that tribological diagnostics are crucial for ensuring the safety of flight operations. Their study highlights the role of periodic tribological testing in maintaining the operational safety of aircraft engines through lubricant degradation analysis and wear detection. Such diagnostics help prevent failures by allowing real-time monitoring and risk management in aero-engines, thereby enhancing flight safety and engine longevity [14].

Tribological failures, such as fatigue of engine components, are a well-documented cause of accidents in the aviation industry. May (2010) presents case studies involving fatigue failures in aircraft components, including engine bearings and turbine blades. These failures were directly linked to the fatigue of tribological elements, such as roller bearing cages, which resulted in accidents. The study underscores the importance of understanding wear mechanisms and fatigue

to prevent such failures, which, although not always life-threatening, can lead to significant operational and economic losses [21].

The consequences of insufficient tribological analysis are exemplified in Dundas' (1993) study on gas turbine engine failures. This research highlights a case where an aircraft accident could have been avoided with more thorough tribological failure investigation. Dundas stresses the need for systematic approaches to investigating tribological failures in gas turbines, illustrating that detailed analyses of wear, friction, and lubrication are essential for preventing future accidents and extending engine life [22].

Thus, ongoing advancements in tribological diagnostics, wear prevention, and fatigue management remain paramount for enhancing safety and reliability in the aerospace industry.

Over the past years, Holmberg et al., (2012, 2013, 2014, 2017, 2019) have systematically investigated the global repercussions of friction and wear on energy and the environment. Despite notable advancements, their studies underscore a significant energy loss attributed to friction, particularly prevalent in the transportation sector. The Jost committee's findings in the 1960s suggested that adopting advanced tribological materials and practices could yield economic gains of 1.0% to 1.5% of GDP by reinvesting 2% of these gains [23], [24]. Presently, even less investment is deemed sufficient to achieve more substantial positive impacts through the integration of advanced tribological solutions.

2.1.3. The Critical Role of Coatings in Tribological Systems

While coatings and solid lubricants are critical in reducing friction and wear in mechanical systems, inefficiencies in these coatings can lead to severe wear and compromise safety. Several documented cases highlight the consequences of coating failures, particularly in high-performance applications such as aerospace and automotive industries. For example, tungsten carbide thermal spray coatings, frequently used in aerospace, have been shown to fail due to spallation and cracking, which can lead to decreased engine performance and costly maintenance [25].

Behera et al. (2021) investigated the use of sacrificial Cd and Al coatings on aerospace and automotive-grade steel, noting that although these coatings provided initial protection, their effectiveness diminished with wear. Cd coatings, which acted as a solid lubricant, offered better performance, particularly in varying humidity conditions. However, Al coatings, used as a replacement due to Cd's toxicity, resulted in increased wear rates, especially in dry conditions. The failure of the Al coatings led to significant wear on the steel substrate, raising concerns about long-term safety in aerospace applications [26].

Solid lubricants, such as multi-wall carbon nanotubes (MWCNTs), have been used in tribological systems operating under high temperatures or vacuum environments. While MWCNT coatings initially performed well by reducing friction and wear, their performance deteriorated over time due to structural degradation under mechanical stress. This led to the removal of the lubricant coating, significantly increasing the wear rate and reducing the protective capabilities of the surface. Such failures in high-stress environments demonstrate the need for more robust coating systems in critical applications [27].

Coatings applied via thermal spraying, such as those using tungsten carbide and fluorinated ethylene-propylene (FEP) copolymers, are designed to improve wear resistance in sliding contact applications. However, Marple & Voyer (2001) found that the effectiveness of these coatings heavily depended on the precise optimization of solid lubricant content. Suboptimal formulations led to rapid wear, reducing the coatings' efficiency and increasing the risk of component failure. This highlights the need for precise material engineering to ensure the long-term durability of coatings in industrial environments [28].

In advanced power-generating systems such as gas turbines, traditional solid lubricants often fail under elevated temperatures, leading to significant wear and reduced system efficiency. It is demonstrated that conventional lubricants, such as polymers and laminar solids, were unsuitable for use beyond 450 °C, necessitating the development of new materials like metal fluorides and oxides to maintain lubrication. The failure of these coatings in high-temperature applications underscores the critical role of coatings in ensuring operational safety and preventing material degradation [29].

In complex tribological environments, bonded MoS_2 coatings are used to reduce friction and wear in sliding contacts. Environmental factors, such as high humidity and temperature, led to the oxidation and degradation of the coatings. This significantly reduced their effectiveness in protecting the substrate from wear. The study emphasizes the importance of environmental considerations when designing coatings for high-performance applications [30].

The use of diamond like coatings in engine parts can help achieve the desired efficiency and lower emissions [31]. However, they have limitations, such as cost-effectiveness and their compatibility with certain engine designs and lubrication regimes. Therefore, we introduce photocuring of

graphene oxide as a new coating technology to address these challenges providing a potential improvement of efficiency and reduction of the environmental impact.

2.1.4. Limitations and Challenges in Implementing Graphene-Based Coatings and lubricants

Graphene possesses extraordinary physical properties that contribute to its uniqueness. These properties include exceptional mechanical strength, high thermal and electrical conductivity, remarkable magnetism, and outstanding chemical reactivity [32]. Generally, graphene oxide exhibits a layered structure (Figure. 2.1) and unique properties that make it versatile for various applications. The mechanical strength and light weight of 3D graphene oxide structures make them attractive for engineering applications where non-planar structures are required, indicating a broader scope for graphene oxide in industry [33].

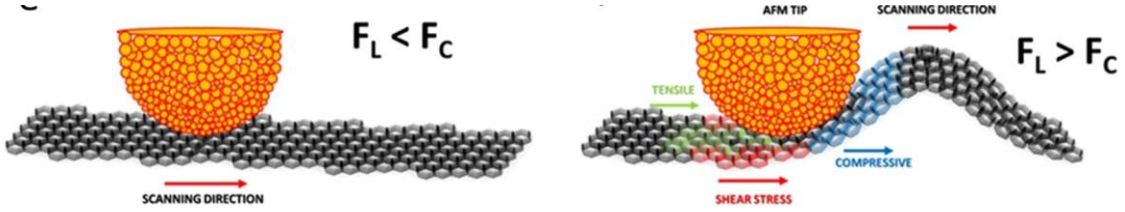

Figure 2.1. Deformation of graphene sheet by tip of atomic force microscope when lateral forces F_L are smaller than the critical force F_C for Euler buckling, the graphene sheet remains planar. Adapted from [34]

In a nanoscale, they exhibit exceptional hardness and adhesion, enhancing durability and performance [35], [36], with increased microhardness, reduced roughness, and improved wear and corrosion resistance [37]. Additionally, graphene exhibits high charge mobility, high Young's modulus value, and a hexagonal lattice structure with sp^2 hybridization, leading to its high conductivity and mobility of charge carriers [38].

Graphene coatings come in several forms based on their material structure, each offering unique properties for specific applications. Common types include nanocomposites, where graphene is integrated into polymer matrices or with other nanomaterials for enhanced corrosion resistance and mechanical strength [39]; layered coatings, which provide impermeable barriers against oxidation [40]. Hydrophobic graphene coatings are used for moisture resistance [41], while biomedical coatings integrate graphene with biocompatible materials for medical implants [42]. Additionally, metal-graphene hybrid coatings improve electrical conductivity and corrosion resistance, making them suitable for electronics and energy storage applications [43]. Graphene-based nanocomposite coatings have emerged as a promising solution for improving the durability and performance of materials in some industries [44], [45], [46], [47]. These coatings offer significant advantages due to graphene's extraordinary mechanical, thermal, and chemical properties. However, despite their potential, graphene coatings face limitations in specific high-demand applications, such as aerospace.

Importantly, the need to reduce CO_2 emissions is driving the demand for materials capable of withstanding extreme conditions such as aircraft engines [48], [49]. Evaluating the Global Warming Potential of commonly used alloys in gas turbine engines has highlighted the importance of material selection in mitigating environmental impacts during aviation engine component production [50], [51]. For example, Shi et al. (2022) introduced a graphene-based nanocomposite copolymer, GO-g-(PMMA-co-PMPS), which demonstrated high durability, transmittance, hydrophobicity, and strong adhesion [4]. Nonetheless, while these properties are promising for some sorts of protective coatings, the research does not provide detailed insights into the coating's performance under the extreme conditions of high temperatures, pressures, and corrosive

environments. This highlights the need for further investigation into the mechanical durability of graphene coatings in these demanding settings.

In marine environments, graphene coatings offer environmental benefits, with improved mechanical properties, corrosion resistance, and thermal stability, reducing recoating needs [52]. They inhibit biofilm development, making them potential antifouling coatings [52], [53]. These coatings are eco-friendly, with excellent anti-corrosion performance, simplifying maintenance and cutting costs [54] but they are still limited to this application.

Graphene liquid lubricants have addressed the inadequacies of current coatings in certain types of extreme environments by being highly-durable and protective [5] but the applications of liquid lubricants is still limited for certain conditions. Solid graphene lubricants offer reduced friction and wear, making them suitable for certain limited macroscale industrial application [55], however as the graphene sheets are loosely packed with random orientations on the substrate, even though they withstand high loads, they cannot be used in applications involving extreme thermal pressures.

Despite these impressive properties, graphene coatings still face challenges in certain large-scale applications. One significant challenge is the self-assembly of graphene sheets into macroscopic structures, which could potentially unlock broader industrial applications. This study aims to explore this aspect tribologically.

2.1.5. Tribology and the Quest for Sustainable Coating Materials

Developing materials with enhanced wear resistance remains a critical area of research. Understanding the relationship between material properties and wear mechanisms is essential for designing new alloys and composites that can withstand extreme conditions [9]. The integration of tribology with smart technologies, such as sensors and IoT, can lead to advanced monitoring and

maintenance systems. These technologies can provide real-time data on friction, wear, and lubrication, enabling predictive maintenance and reducing downtime [56].

2.2. Innovative Materials for Advanced Tribological Systems

2.2.1. Liquid Crystals: Properties and Applications

Liquid crystals are a unique phase of matter that exhibit properties of both liquids and crystals, flowing like ordinary liquids while possessing crystalline characteristics [57]. In the context of liquid crystals, isotropic, biphasic, and nematic phases (Figure. 2.2) refer to different levels of molecular order [58]. In the isotropic phase, molecules are randomly oriented without long-range order, behaving like a typical liquid. The biphasic state is a transitional phase where both isotropic (disordered) and nematic (ordered) regions coexist. In the nematic phase, molecules align along a common axis (the director), maintaining fluidity but exhibiting long-range orientational order. These phases demonstrate varying degrees of molecular alignment, influencing their optical and mechanical properties. They are structurally diverse, with various types such as lyotropic, polymeric, thermotropic, and discotic [57].

Crystalline characteristics in liquid crystals refer to their unique structural properties, which are a blend of both liquid and solid states. Liquid crystals, like nematic, smectic, and cholesteric phases, exhibit some level of molecular organization akin to crystals, while maintaining the fluidity of liquids. For example, in nematic liquid crystals, molecules align along a particular direction but remain free to move, similar to a fluid. This intermediate structure allows liquid crystals to exhibit anisotropic properties, such as birefringence, which are typically associated with solid crystals. The ability of these materials to self-organize into various phases and their responsiveness to external

fields (e.g., electric or magnetic) give them their characteristic optical and mechanical behaviors, which are leveraged in applications like liquid crystal displays (LCDs) and sensors [59].

Liquid crystals have found extensive applications in fields like optics, photonics, and chemical industries due to their exotic electromagnetic properties and varying molecular structures [60]. These materials have been utilized in the development of metamaterials, biomedicine applications like tissue identification and drug delivery, and even in the creation of photonic crystals for optical devices [57]. We are going to use the order of liquid crystals and convey it to the solid-state order to obtain the mechanical and thermal strength and the stability.

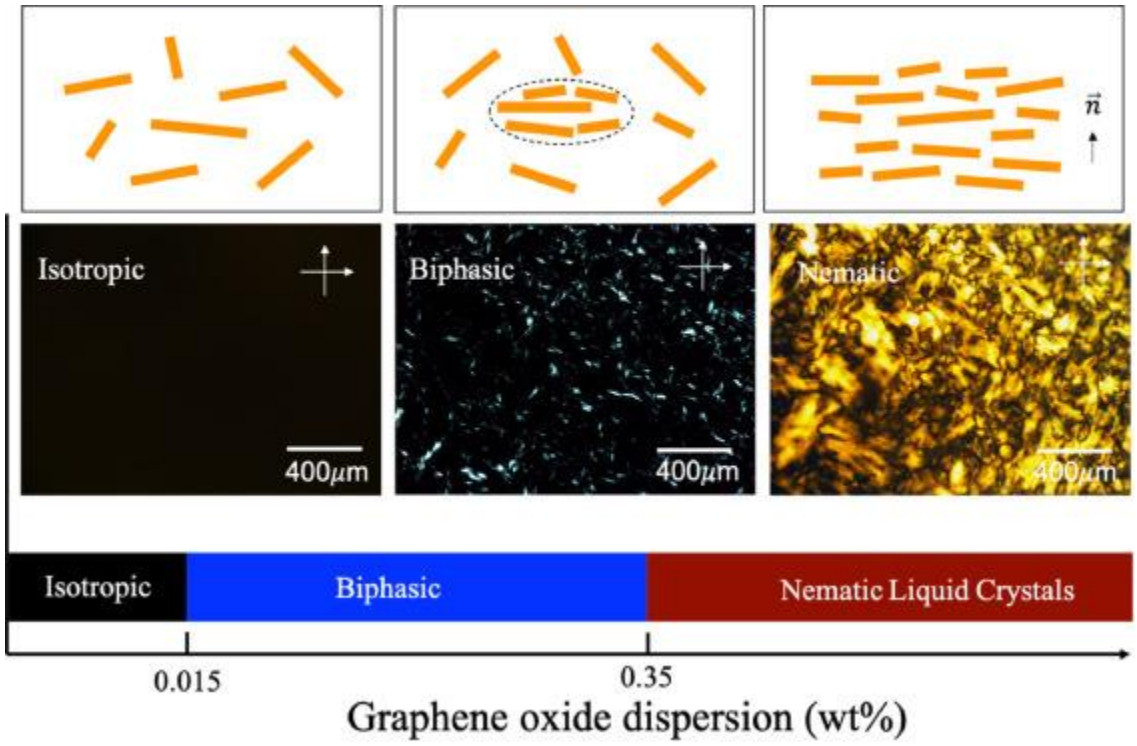

Figure 2.2. Lyotropic liquid crystalline phase diagram of GO in aqueous dispersions. Typical optical textures and GO sheet orientation in isotropic, biphasic, and nematic liquid crystalline phases are shown at the top. Adapted from [58]

2.2.2. Photopolymerization

In this work, we aim to utilise the self-organization of liquid crystals and transfer this inherent order into the solid state through photopolymerization. By doing so, we can achieve mechanical strength, thermal stability, and enhanced durability—key properties required for applications in highly demanding environments. The ability to convert the liquid crystalline order into a robust, solid structure opens up new possibilities for the development of advanced coatings that not only resist wear and friction but also withstand extreme conditions, making them ideal for aerospace and other high-performance industries.

Photopolymerization is a process wherein light induces a chemical reaction that alters the material's properties, such as transitioning from liquid to solid, changing solubility, enhancing adhesion, or modifying refractive index [6]. Since its inception with polyvinyl cinnamate, used in printing plates, photopolymerization has found numerous applications, including the production of printed circuit boards, photocurable coatings, and 3D printing via stereolithography [6], [61]. Photopolymerization is often preferred over thermal polymerization, particularly in dental applications, due to its lower energy requirements and more comfortable process [62]. However, there remains a challenge in controlling the specific wavelengths necessary to initiate photopolymerization reactions effectively.

Photopolymerization mechanisms are primarily categorized into free-radical and cationic types. In free-radical photopolymerization, radicals are generated through photoinitiation, involving processes such as alpha cleavage or hydrogen abstraction [63]. Conversely, cationic photopolymerization involves the decomposition of an initiator to form cationic species, which then generate protons to open epoxide rings and initiate polymerization [64].

2.2.2.1. Free-Radical Photopolymerization

The radical photo-initiation of acrylic monomers has been extensively studied, utilizing various initiators, including semiconducting nanoparticles [61]. For instance, butylmethacrylate can be photopolymerized using ZnO quantum dots and other nanoparticles like CdS, which function via free radical photopolymerization. When these semiconducting materials absorb light at their bandgap energy, electron-hole pairs form, with the electron acting as a free radical that initiates acrylate polymerization [65].

2.2.2.2. Cationic Photopolymerization of Epoxy

This thesis focuses on the cationic photopolymerization of epoxy, which requires specific cationic initiators. Onium salts, first developed by Crivello, are widely used as cationic initiators. The effectiveness of these initiators in photopolymerization depends on the properties of both the anion and the cation in the salt. The anion determines the acid strength and efficiency of the reaction, while the cation, which absorbs the light, influences the photochemical properties, including the absorption wavelength, quantum yield, and thermal stability [66].

The mechanism of cationic photopolymerization involves the absorption of light by the cation, leading to the generation of protons that open the epoxide rings and initiate polymerization [64]. This process is illustrated in Figure 2.3:

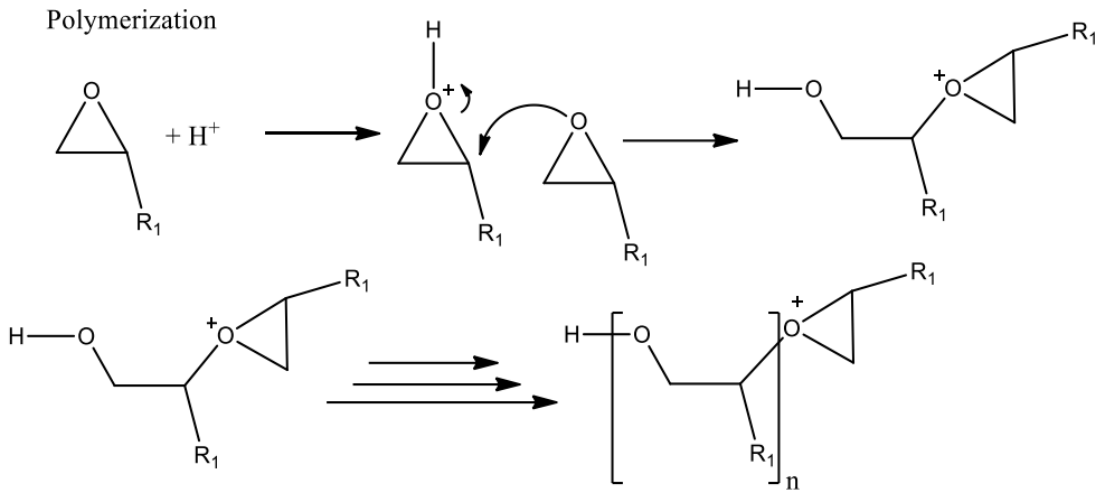

Figure 2.3. Cationic polymerization of epoxide group in graphene oxide. Adapted from [67]

The efficiency of this process is influenced by the light wavelength, with current photo-initiators typically responding to UVA (315-400 nm) and UVB (295-315 nm) light, which constitutes about 6% of solar intensity at sea level [8]. However, exposure to UV light leads to degradation of the material, causing issues such as brittle fracture and the release of toxic volatile organic compounds (VOC) into the environment [61].

Chapter 3. Thesis Objectives

This literature review highlights the limitations and emerging solutions in wear mitigation, setting the stage for the exploration of graphene-oxide liquid crystal coatings as a promising alternative. The review's insights directly inform the objectives of this thesis, which focus on developing and assessing these innovative coatings to improve wear resistance and tribological performance in critical applications. Therefore, our objective is:

- ✓ **To Develop a Novel Coating Technology with enhanced tribological properties**

Investigate the use of photocured graphene-oxide liquid crystal coatings as an alternative to traditional coating methods. Develop a methodology for applying these coatings on titanium grade 5 and assess their effectiveness in improving wear resistance and tribological performance.

- ➢ In order to achieve this objective, we must perform the following:

- Evaluate the Tribological Performance of Coatings

Conduct dry sliding wear tests to compare the tribological behavior of graphene-oxide coated samples with bare titanium substrates. Analyze the friction and wear performance of the coatings, particularly focusing on the effects of annealing.

- To Characterize the Coatings Thoroughly

Utilize various characterization techniques, including confocal laser microscopy, scanning electron microscopy, micro-Raman spectroscopy, and atomic force microscopy, to examine the physical and chemical properties of the coatings. Assess the structural integrity and durability of the coatings under different conditions.

By addressing these objectives, the thesis aims to advance the field of tribology and contribute to the development of sustainable and high-performance coating solutions for industrial applications.

Chapter 4. Photocured graphene-oxide liquid crystal coatings for improved tribological performance

4.1. Abstract

Wear-related challenges in mechanical components, particularly in industries like aerospace, require innovative solutions for improved performance and sustainability. Traditional coating methods such as physical vapor deposition and high-velocity oxygen fuel have limitations, prompting the exploration of alternative approaches. Here we explore the use of graphene oxide liquid crystals and photocuring to produce enhanced coating. Graphene itself has exceptional properties but the challenge of extending the behavior to larger scales requires strong bonding between the platelets. By making use of the liquid crystal self-assembly of graphene oxide in alcohol we can order the platelets densely on the substrate and then create permanent bonds through photocuring significantly enhancing durability and tribological performance. We have achieved a remarkable reduction of 72% in the friction coefficient as compared to the bare substrate. Experimental results underscore the efficiency of thin, annealed graphene oxide films in protecting the substrate, reducing wear, maintaining low friction.

➢ Keywords: Coatings - Graphene Oxide - Friction - Wear- Photocuring - Liquid Crystals

4.2. Introduction

Wear between mechanical components, is a significant issue that has implications for the environment, cost, and most importantly, the safety of people in various industries (e.g. aerospace, automotive). More specifically, wear leads to the gradual removal or deformation of materials, resulting in the need for maintenance and repair, which can be costly [68], [69]. In the aerospace industry, premature wear can have severe consequences, as it can lead to catastrophic failures and operational breakdowns that can impact productivity and safety [70], [71]. Conventional internal combustion engines have significant energy losses due to heat and friction [31]. Coatings are commonly used to enhance tribological behavior (i.e. reduce wear and friction), including those produced by physical vapor deposition (PVD) [72], high-velocity oxygen fuel (HVOF) [73], and electric arc spray [74].

Within internal combustion engines, 15% of energy consumption is due to frictional losses, contributing to millions of tons of CO_2 emissions annually [75], [76]. Modern tribological strategies emphasize the significance of low-friction surfaces and enhanced lubrication to address environmental concerns by optimizing fuel efficiency, and minimizing emissions [77], [78], [79]. Therefore, we introduce in this work a strongly bonded graphene-oxide coating as a potential candidate for such applications.

Multilayer and high-entropy alloy-based coatings are being developed as a means to protect structural components and extend their operational lifespan, reducing the need for critical raw materials in manufacturing [80], [81], [82], [83], [84]. Drawbacks include limitations with available production methods and high costs [85], [86].

The use of diamond like coatings in engine parts can help achieve the desired efficiency and lower emissions [31]. However, they have limitations, such as cost-effectiveness and their compatibility with certain engine designs and lubrication regimes. Therefore, we introduce photocuring of graphene oxide as a new coating technology to address these challenges providing a potential improvement of efficiency and reduce environmental impact.

Graphene coatings are extremely promising, as they are highly-durable, protective [4], [5], [55] and provide excellent tribological performance [35], [36], [37], [53], [55], including reduced friction [36]. Graphene based coatings have been shown to be resistant to acid/alkali, salt, ultraviolet light [4] and thermally stable [40]. However, their suitability in demanding conditions, including high pressures and mechanical stresses remains uncertain. Graphene itself exhibits unique properties [44], [45], [46], [47] but the challenge is always extending those properties to the macroscale. To extend the properties to larger scales, we need to order and bond the graphene particles. Ordering can be achieved with different methods including liquid crystals and self-assembly [87]. Such methods typically involve secondary bonding between graphene sheets however we will explore the use of covalent bonds between the graphene particles.

Self-assembly involves the spontaneous organization of building blocks into nano- or micro-structures like micelles (particles soluble in water) and liquid crystals [88]. Liquid crystals exhibit both liquid-like properties and crystal-like order [87] making them an interesting intermediate state for forming coatings. The process of self-assembly initiates with an isotropic suspension of graphene oxide sheets possessing amphiphilic properties. These sheets interact, leading to their stacking and the subsequent formation of liquid crystals exhibiting nematic [89], columnar [90] or chiral nematic [89] ordering. Hydrogen bonding, ionic bonds, and Π- Π interactions, may coexist within the same system [91], [92]. Macroscopic structures, such as paper and fibers, arise from

self-assembly combined with another processing step [93] such as wet-spinning, freeze-drying, and filtration, which maintain the ordered structure observed in the liquid crystal phase.

Photocuring of cast suspensions of self-assembled graphene oxide has been proven to be a powerful technique to create macroscopic structures allowing for thicker coatings [94]. The photocuring process does not require high temperatures or sophisticated infrastructure other than a UV light source and is thus a promising approach to producing enhanced tribological coatings. This simplicity and effectiveness can save manufacturing costs. Importantly, photocuring allows the formation of strong, covalent bonds between graphene oxide platelets [94] but also, we will show, between the coating and the substrate. Thereby, our approach may enhance the overall durability and effectiveness of the coating, potentially for demanding conditions. To avoid interference of water with the cationic photocuring reaction of epoxy, we adopted the approach suggested by Riad et al. [94] following Jalili et al. [95] to prepare photocured graphene oxide liquid crystals dispersed in 1-phenylethanol (1-PtOH). The epoxide groups situated on the basal planes of graphene oxide sheets, when organized into an ordered liquid crystal, can undergo crosslinking to form a solid structure with good mechanical properties at the macro scale [94]. Strong adhesion between graphene and substrates plays a crucial role in enhancing the formation of a tribologically enhanced coating [55]. Adhesion between graphene and the titanium substrate allows for the formation of a dense layer of graphene-containing tribo-film within the sliding interface, leading to reduction of friction and wear on the substrate surface [55]. This effect may be amplified when the graphene platelets are well-ordered, enhancing friction and wear reduction, as our work proposes.

The epoxide groups on graphene oxide enable the formation of strong covalent bonds [96], allowing for durability and efficacy of graphene coatings. We use this idea to apply graphene oxide coating on a titanium substrate and demonstrate that they exhibit desirable tribological properties

directly linked to their structure and morphology. This study introduces a pioneering approach to enhance the tribological properties of graphene oxide coatings on titanium components, crucial for industrial applications including aerospace. By taking advantage of liquid crystals and photocuring, the research achieves strong, covalent bonds between graphene layers in a coating that is also strongly adhered to the substrate, ensuring durability. This innovative method not only improves resistance to friction and wear thus promoting environmental sustainability and marking a significant advancement in coating materials science and engineering.

4.3. Experimental Methodology

4.3.1. Materials

Titanium grade 5 substrates (1 in x 1 in) are used. Graphene oxide powder (S Method, product #: GNOS0010), obtained from ACS Materials, was used as received. Additionally, 1-phenylethanol (98%) and bis(4-methylphenyl)iodonium hexafluorophosphate (photoinitiator, 98%), from Sigma Aldrich, were used without further modification.

Prior to casting the coatings, surface roughness of the substrates was assessed using a profilometer with recorded values ranging from 0.5 to 0.7 μm. Graphene oxide alcohol dispersions were then prepared according to a method adapted from Riad et al. [94]. As shown in Scheme 1, a 2 wt.% solution of photocuring initiator in alcohol was used to prepare 5 suspensions consisting of 9 g of liquid and 5 incremental weights of graphene oxide (0.04g, 0.08g, 0.12g, 0.16g and 0.20g) to form concentrations of 0.44, 0.88, 1.31, 1.74 and 2.17 wt.% of graphene oxide suspended in alcohol. Immediately after stirring and sonication the dispersions were evenly cast onto titanium substrates using a pipette, resulting in ten coated samples. These samples underwent photocuring for 48 hours under a benchtop UVA lamp (Model: UVP XX-15 L, peak emission: 365 nm, light intensity at

sample surface: 4 mW/cm^2) until solidified. Finally, one sample at each concentration was annealed at 190 °C for 2 hours. See Figure S1 from the supporting information for images of the specimens.

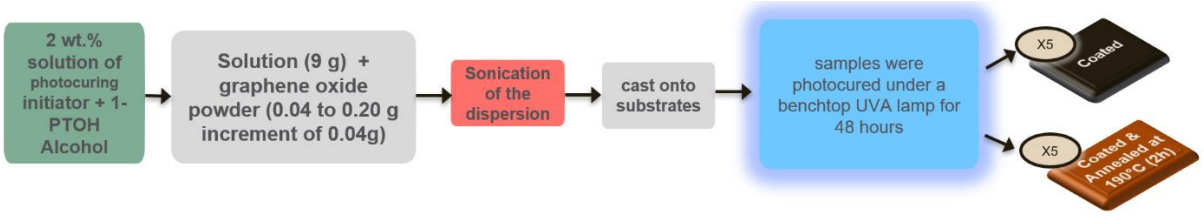

Scheme 1. Process flowchart for the preparation of coated titanium samples

4.3.2. Coating Thickness

To evaluate the thickness of the coatings, surface profiles are obtained before and after coating using a confocal laser microscope (Model: Olympus LEXT 4000) (Figure 4.1). Since equal volumes of dispersion were cast on all substrates, the remaining mass of graphene oxide after solidification and evaporation of alcohol is relative to the dispersion concentration. Thus, the higher the graphene oxide concentration, the thicker the coating. The annealed coatings are thicker than the untreated coatings due to swelling during evaporation.

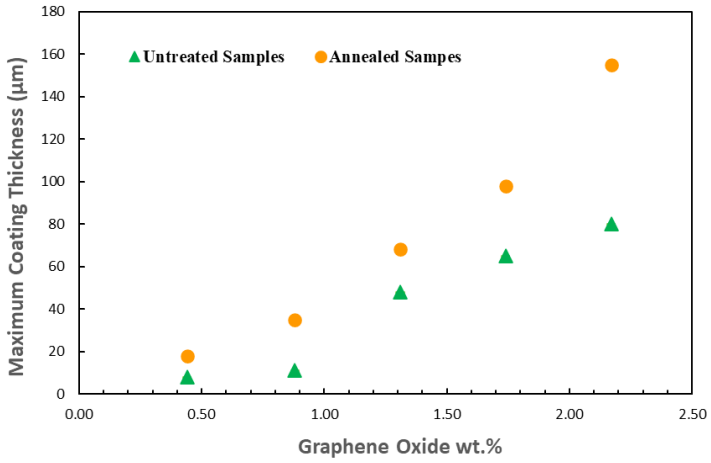

Figure 4.1. Coating Thicknesses Plotted Vs. Graphene Oxide Content

4.3.3. Dry sliding wear testing

The tribological performance was evaluated using a ball-on-disc (TRB³ | Anton-Paar tribometer) under reciprocating dry sliding wear with the conditions specified in Table 1 (3 repeats).

Table 1. Sliding wear test parameters

Sliding Wear Test Parameters	Values
Load	5 N
Stroke Length (Track Length)	10 mm
Frequency	1 Hz
Number of Cycles	5000
Sliding Speed	3.14 cm/s
Sliding Distance	100 m
Counter face	Al_2O_3
Counter face Ball Diameter	6.35 mm
Temperature	25°C to 28°C
Relative humidity	18% to 22%

4.3.4. Characterization

A Nikon Ti polarized light optical microscope (POM) was used to determine the degree of order of the graphene oxide liquid crystals in the dispersions. The wear profiles and the counter faces were analyzed using a confocal laser microscope (Olympus LEXT 4000). Average wear profiles are presented from 20 cross-sections across 2 tracks. Scanning electron microscopy (SEM) (SU3500, Hitachi) was used to examine the worn surface morphology. EDS was also performed using the Oxford Aztec X-Max50 SDD system of the SEM. Raman spectra were recorded using a Renishaw spectrometer at room temperature, with a solid-state laser operating at 532 nm and a 100× objective

at 10% power from 1200 cm^{-1} to 2100 cm^{-1}, calibrated using a silicon standard (520 cm^{-1}). Each spectrum was obtained from at least three different spots in the desired region to ensure consistency. The atomic force microscope *Tosca*™ 400 by Anton Paar is employed to measure the pull-off force on worn surfaces to determine maximum adhesion force [97].

4.4. Results and discussion

4.4.1. Dispersion Characteristics

Polarized light microscopy of our graphene oxide dispersions is used to verify the formation of a liquid crystalline structure (Figure 4.2), in this case nematic phase. Prior findings show that at 1.13 wt.% graphene oxide in 1-PTOH, the sheets form an anisotropic ordering [94]. The birefringence observed in all dispersions indicates ordering, consistent with liquid crystal structures reported in literature [94], [98]. The more birefringence (i.e. the less black) in the image indicates more ordering [58], [98].

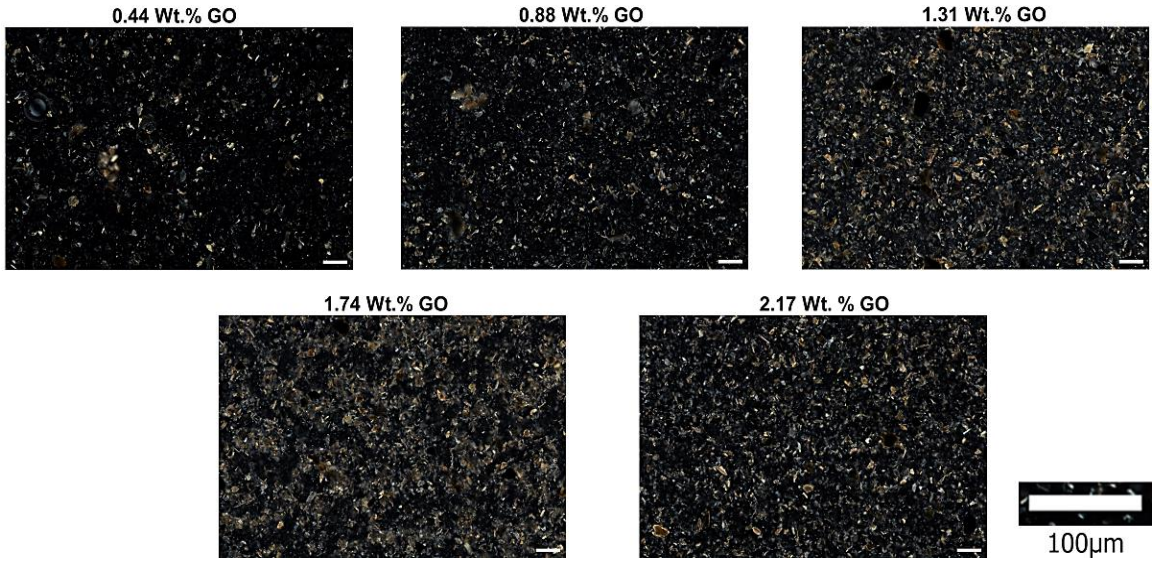

Figure 4.2. Crossed polarizer micrographs for all graphene oxide dispersions in 1-PTOH-alchohol

By calculating the birefringent area fraction from the micrographs (Figure 4.2) we can estimate the degree of ordering or the amount of nematic to isotropic phases (Figure 4.3) [98], [99]. We observe that for most of the dispersions, the degree of ordering increases with graphene oxide content indicating a biphasic system of isotropic and nematic. At the highest graphene oxide content, we observe a decrease in the area fraction, possibly due to a phase transition to another phase structure. After photocuring, crosslinking, and solidification, covalent bonds form between the graphene oxide particles. The ordering in the dispersion results in ordered coatings which assists in the formation of covalent bonds between particles during curing.

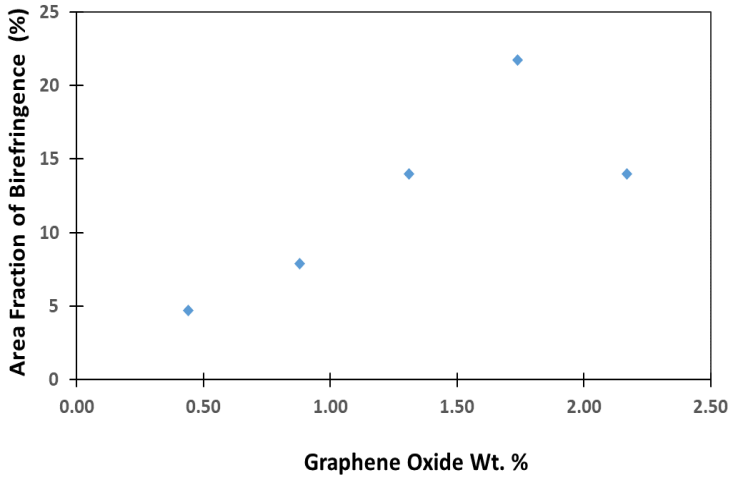

Figure 4.3. Percentage of Crystal Order within Dispersions Vs. Graphene Oxide Wt. %

4.4.2. Coating Characteristics

Figure 4.4A shows the average steady-state friction coefficient of our coatings as a function of graphene content for the untreated and annealed samples, compared to that of the bare substrate. Figure S3 presents examples of experimental data (friction coefficient as a function of wear cycle). The untreated samples exhibit a friction coefficient lower compared to that of the bare substrate at

graphene contents above 1.31 wt.%. The annealed samples exhibit a consistent low friction coefficient irrespective of the graphene oxide content; with a reduction of up to 72% as compared to the bare substrate. Importantly, the untreated sample containing 1.31 wt.%. graphene oxide behaves in a transitional manner. In some cases, this coating exhibits a low friction coefficient whilst in others, it was close to that of the bare substrate, with no intermediate behavior observed. This is represented in the figure with the large standard error bars.

Figure 4.4B. shows the maximum wear depth for our two series of samples. In this graph we place the surface of the substrate at zero and measure relative to that. Therefore, any value below zero, indicates that the alumina counter face has worn into the substrate and accordingly, the coating has not protected the substrate. This is the case for the untreated samples with the lowest 3 graphene oxide contents which also exhibit the highest steady state friction coefficients (Fig. 4.4A). The wear depths for these samples are above the bare substrate wear depth (~32 μm), indicating some wear resistance is provided by the coating. Conversely, positive values in Figure 4.4B indicate that the substrate is not worn and was therefore protected by the coating. The coating is worn to some extent, but the alumina counter face has not reached the substrate. This is the case for the untreated samples at higher graphene oxide contents and for all the annealed samples. From Figure 4.4, we conclude that annealing results in an effective coating in terms of wear behavior and that in the absence of annealing only higher graphene contents provide for effective coatings.

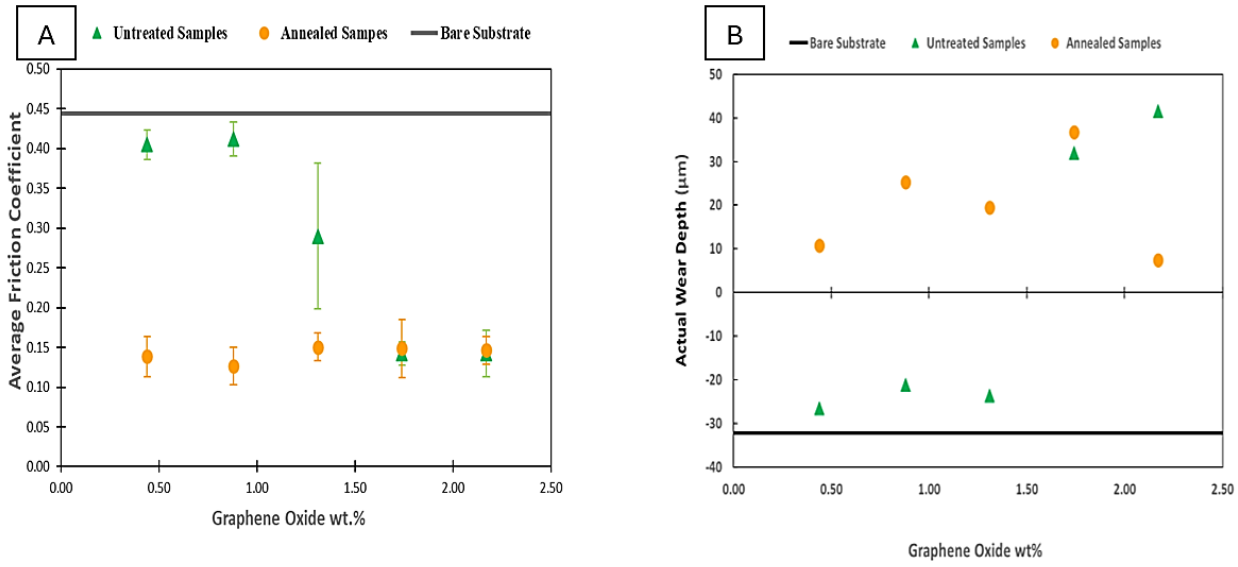

Figure 4.4. Tribological Properties of Coatings. A - Average friction coefficient and B- Maximum wear depth as a function of graphene content (extracted from Figs 4.5 and S4)

Figure 4.5. shows average wear profiles from multiple cross sections of the wear tracks. In this figure we focus on the wear profiles of the highest and the lowest graphene contents for both the untreated and annealed sample series along with those of the bare substrate. These results are consistent with the results for the other specimens which are presented in the Supporting Information (Figure S4). The profiles are plotted such that they are vertically shifted above the zero position of the unworn bare substrate by adding the coating thickness measured independently from this experiment (Figure 4.1) and presented in Figure 4.5. From Figure 4.5A, we see that the untreated sample with the lowest graphene oxide content, 0.44 wt.%, was worn through the coating and into the substrate. In contrast, for the other samples shown here, the substrate was untouched.

We can also infer the wear mechanism from these profiles, ploughing or abrasive wear in the case of the untreated samples and brittle fracture or fatigue wear in the case of the annealed samples. A curved wear valley between two pile-ups is characteristic of abrasive wear [100] or adhesive wear

of a deformed thick coating. A valley with a flat bottom and no obvious pile-ups is characteristic of fatigue wear [101]. If a malleable coating is too thin, then abrasive wear results in damage to the substrate as we see in the case of the untreated sample with the lowest graphene content.

With hard coatings, such as the annealed samples, fatigue wear results in coating removed through brittle fracture. The thicker the coating, the more coating is removed but for all the annealed samples, the substrate was protected. During annealing, thicker coatings tend to become more disordered and porous, which contributes to an increase in their overall thickness. This is driven by evaporation of solvent, results in a less dense structure. The higher the graphene content, the more opportunity for covalent bonds to form between the layers and therefore we expect increased hardness and brittleness. Note that in our study the coating thickness increases with graphene content. From the wear tracks we conclude that annealing increased the hardness of the coating and likely its adhesion to the substrate allowing for protection of the substrate even at very low graphene contents. Conversely, without heat treatment, the coating is more malleable, and substrate protection requires thicker coatings.

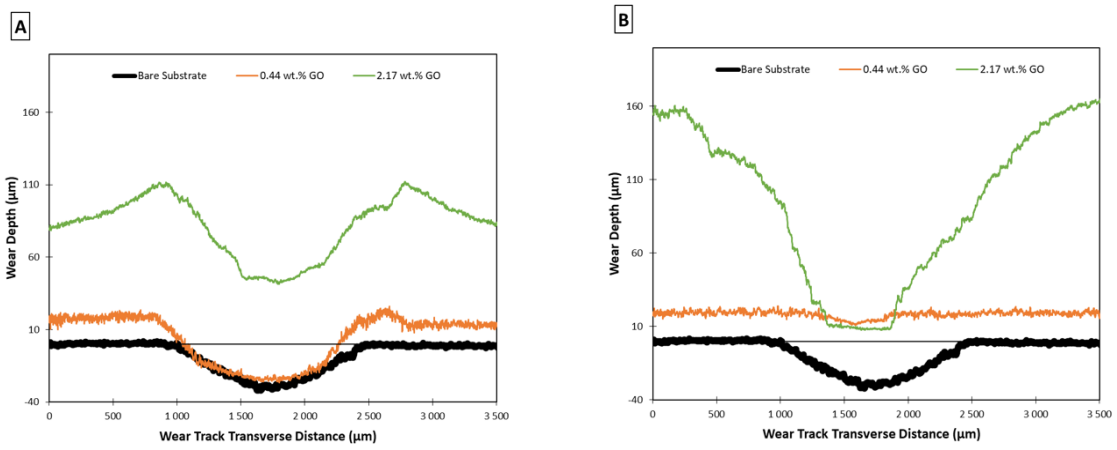

Figure 4.5. Wear Profiles plotted for highest and lowest graphene contents along with the bare substrates. A-Untreated Samples (abrasive wear) and B-Annealed Samples (fatigue wear)

Figure 4.6 shows the alumina counter faces after the sliding wear tests (5X mag.). Substrate material (titanium and its oxides) is transferred to the alumina counter face in the wear tests of the bare substrate, and the untreated coated samples at the 3 lowest graphene oxide contents. This indicates that the coating was completely removed for these 3 samples. No such transfer is observed on the counter faces from the wear tests of the other coated samples. Combined with the wear tracks (Fig 4.5 and Fig S4), this indicates that the substrate remains protected by a thin layer of the coating. These observations are consistent with the high friction coefficients (Figure 4.4A) exhibited by the 3 coatings, which are very close to that of the bare substrate. In alignment with the friction coefficients, the untreated sample containing 1.31 wt.%. graphene oxide behaves in a transitional manner. In some tests, a large transfer layer is observed on the alumina counter face, whilst in others no such transfer is observed, with no intermediate behavior exhibited. See Figure S5 in Supporting Information.

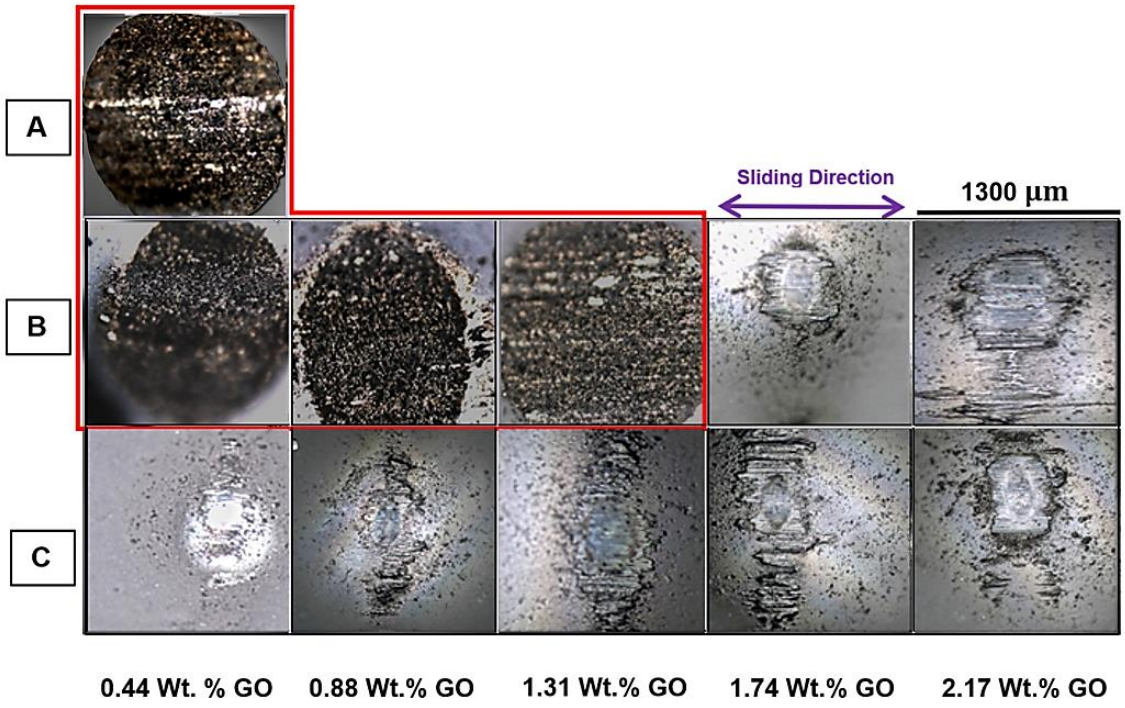

Figure 4.6. Worn Alumina Counter faces at 5X magnification. A-Bare substrate, B-Untreated Samples and C-Annealed Samples. Red box indicates contact with titanium substrate.

Figure 4.7 shows SEM microphotographs of the surface within the wear tracks on the bare substrate and selected coated samples, comprising the highest and lowest graphene oxide contents, for both series. The main observation from the SEM microphotographs is that the bare substrate and the untreated sample containing the lowest graphene oxide, 0.44 Wt.%, act in a ductile manner exhibiting abrasive wear. Conversely, all other samples shown exhibit adhesive and/or fatigue wear. Elemental analyses (Figures S6 and S7 in supporting information) confirm that dark areas on the samples exhibiting fatigue wear are graphene oxide coating remaining on the surface; whilst lighter, grey, regions appear to be titanium and its oxides. In fact, we will demonstrate with Raman spectroscopy (Fig. 4.8) that the light grey areas retain very thin layers of graphene coating.

The bare substrate and the untreated sample with the lowest graphene oxide content (Fig. 4.7A) have scratches parallel to the sliding direction, clearly indicating a ductile material experiencing 2-body abrasive wear [102]. Hard particles that were initially displaced from the surface cause 3-

body abrasion leading to tears and ruptures and the small light-coloured asperities [102] and therefore increased the friction coefficient.

The scratches have been altered by very small spalls and micro spalls and cracks visible on the coated material in Figure 4.7B. The SEM image shows that an adhesive junction is responsible for material removal. During sliding contact, relative motion and cyclic compressive forces occur. Wear from surface fatigue [101] can be identified by visible fractures and flaking of the material [103].

In Figure 4.7C, we see that large pieces of the coating have been removed on samples containing the highest graphene oxide content. These large pieces are welded to the counter surface following either fatigue wear (annealed specimens) or ductile failure (untreated samples). Our observations in Figure 4.7 are in accord with descriptions presented by Holmberg et al. of the relationships between the coating thickness, hardness and the wear mechanism [104].

The SEM study allows us to understand the wear depth results presented in Figures 4.4B and 4.5 showing more coating material loss during wear for the heigh graphene oxide contents compared to that of the lowest ones. Even though the friction remains low, the wear of this excess coating material is undesirable in a manufacturing context. Therefore, we conclude that in order to maintain low friction and avoid dislodging large amounts of coating, it is better to have thinner annealed coatings produced by lower graphene oxide contents.

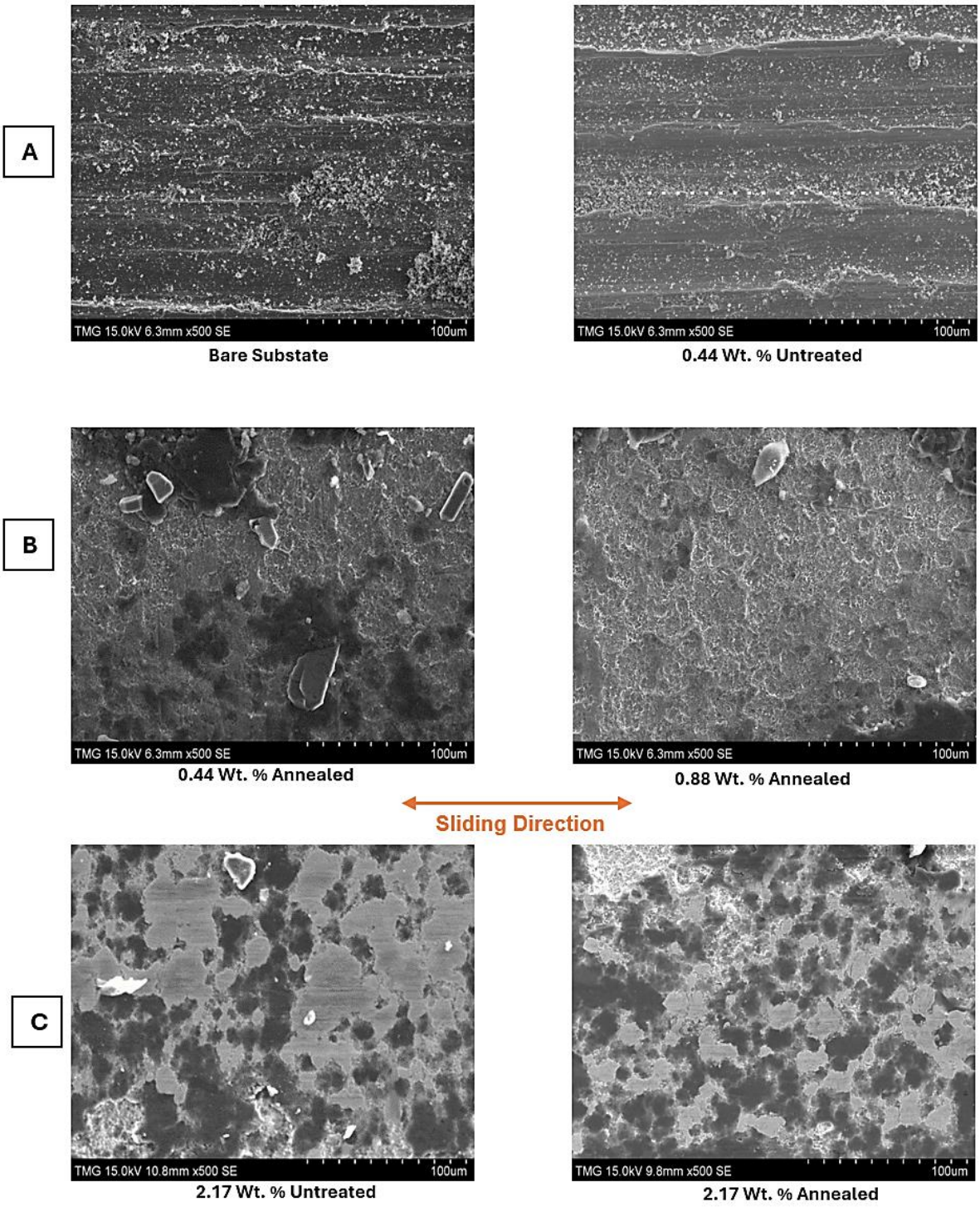

Figure 4.7. SEM micrographs of worn surfaces at 500X magnification A – Abrasive wear of substrate, B – Fatigue wear, C – Fatigue and adhesive wear

Figure 4.8 shows micro-Raman spectra collected from the worn and unworn regions of the surfaces of the coated samples. A typical Raman spectrum of graphene oxide exhibits a G band at 1600 cm^{-1}, and a D band at 1350 cm^{-1} approximately [105]. The G and D bands originate from the stretch (E2g) and breathing (A1') vibrational modes of the six-membered rings in the two-dimensional graphene plane [106], [107].

The observations indicate that graphene oxide is present on all the worn surfaces except for the untreated coatings with the 3 lowest graphene oxide contents. This explains the reduction of friction coefficient for all the other samples and higher friction coefficient for these three. Similarly, as in the discussion of Figure 4.4, these three samples were worn through the substrate as the graphene oxide coating was completely removed during the sliding wear test.

With the presence of graphene oxide on worn surfaces, we confirm that a thin layer of graphene oxide is strongly bonded to the substrate leading to a wear resistant robust coating. The graphene oxide sheets in this thin layer form bonds with the oxide groups on the titanium surface via the same mechanism as the crosslinking between the sheets [94].

In the case of the 3 untreated samples of the lowest graphene oxide contents there is insufficient bonding to form a robust coating. These coatings are soft and thin and can be completely ploughed away from the substrate surface under the effect of the reciprocating motion. With the soft, thick coatings, i.e. the untreated higher graphene oxide contents, a dense tribo-film of graphene oxide is formed with high adhesion to the titanium substrate, under the normal, sliding load. This results in the reduced friction.

Graphene oxide layers are present on the worn surface of all the annealed samples. This is due to the increased coating hardness which results from increased bonding forming between the graphene

oxide layers, and to the substrate during annealing, regardless of the coating thickness. The tribo-film effect during the wear testing is also likely playing a role here [55].

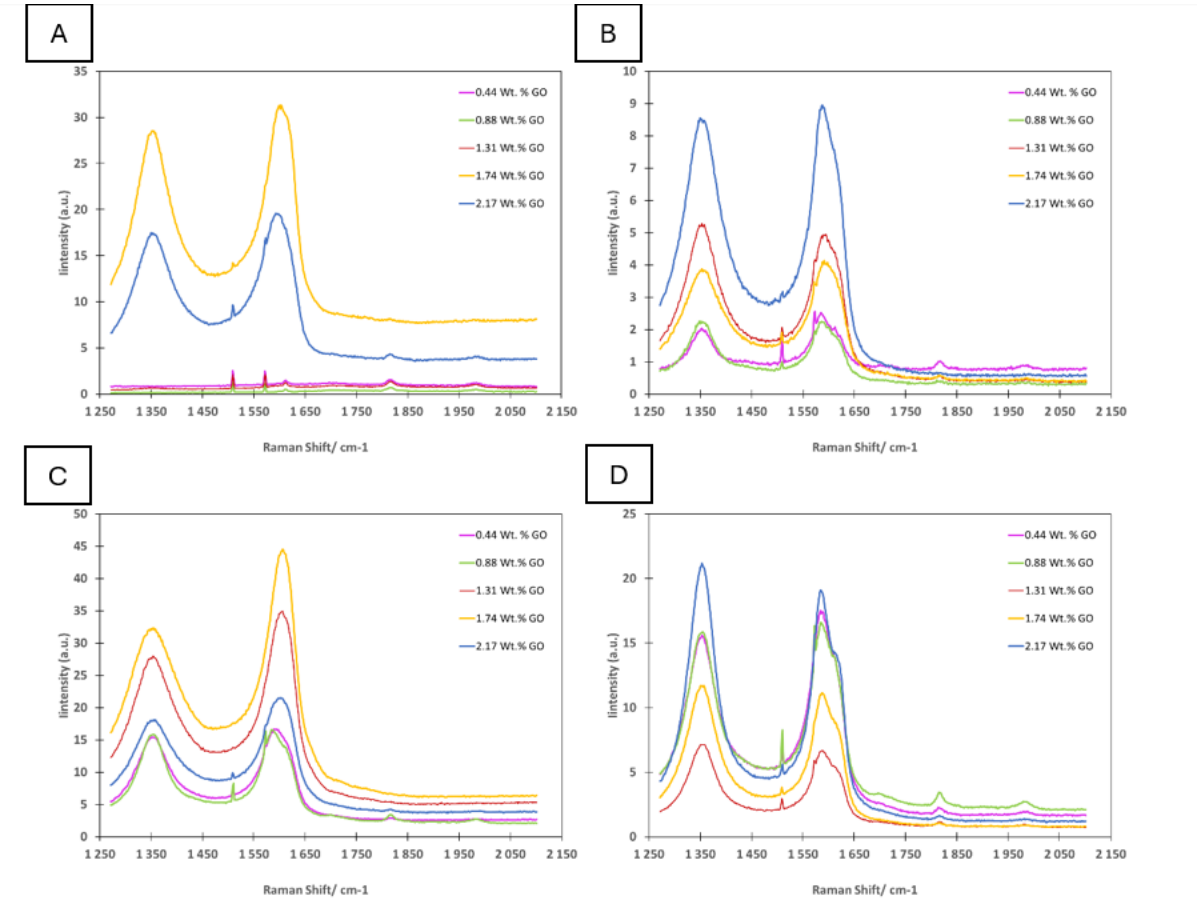

Figure 4.8. Micro Raman spectroscopy of: A-Untreated samples within wear track, B- Untreated samples on coated surface, C-Annealed samples within wear track, D- Annealed samples on coated surface

The ratio between D and G bands in the Raman spectra of graphene, I_d/I_g, gives insight into the number of defects or disorder. [108] In the case of graphene oxide, the oxygen-containing functional groups on the surface of the graphene platelets introduce defects and modify the electronic structure, leading to an increase in the I_d/I_g ratio [109] relative to that of graphene. The exact relationship between the I_d/I_g ratio and the oxygen content of graphene oxide depends on the

synthesis method and the degree of oxidation, but generally, a higher oxygen content leads to a higher I_d/I_g ratio [109], [110].

Figure 4.9 shows the I_d/I_g for the worn and unworn surfaces of the coated samples. As discussed previously, the data are absent when the coatings are completely worn. However, when a thin-graphene-containing tribo-film is formed due to the wear test, i.e., within the worn surfaces, the degree of order is higher than that of the coatings outside the wear tracks. This is true in both sets of samples and is indicative of the ordering of the platelets in the vicinity of the substrate and the relatively less ordering at the surface of the coatings. These observations are consistent with our discussions of the Raman spectra in Figure 4.8. The ordering close to the substrate is due to both the induced liquid crystallinity prior to curing and the formation of the tribo-film during wear.

On the surface of the annealed coatings, we see greater disorder (higher I_d/I_g) due to the rapid release of hydrates and adsorbed alcohol during annealing. There might also be a removal of oxygen-containing functional groups, along with a restoration of sp^2 hybridized carbon bonds occurring, during annealing. This leads to a structure more characteristic of reduced graphene oxide [108] and an increase in the I_d/I_g ratio. Removing any adsorbed substances leads to a dramatic reduction in the interlayer spacing [94], which makes the material more tightly packed and more rigid but more prone to defects [111].

Gases trapped within the intermediate layers in the coating would result in the creation of larger scale defects and the introduction of stress concentrators into the graphene oxide structure, which weakens its mechanical strength [112]. Therefore, although the restoration of sp^2 hybridized carbon bonds can enhance its mechanical strength, the vaporisation of alcohol and other gases can make the material more porous and prone to failure. This porosity and swelling are especially notable in thicker coatings. This became obvious with the annealed sample of the highest graphene oxide

content which exhibited considerable swelling of the coating. This is shown in Figure S2 in the Appendix.

The I_d/I_g ratio on the worn surface shows that the layers closest to the substrate are the most ordered. We can conclude that if we have thinner, annealed coatings, it is favourable for the ordering in terms of the presence of defects and the alignment of platelets.

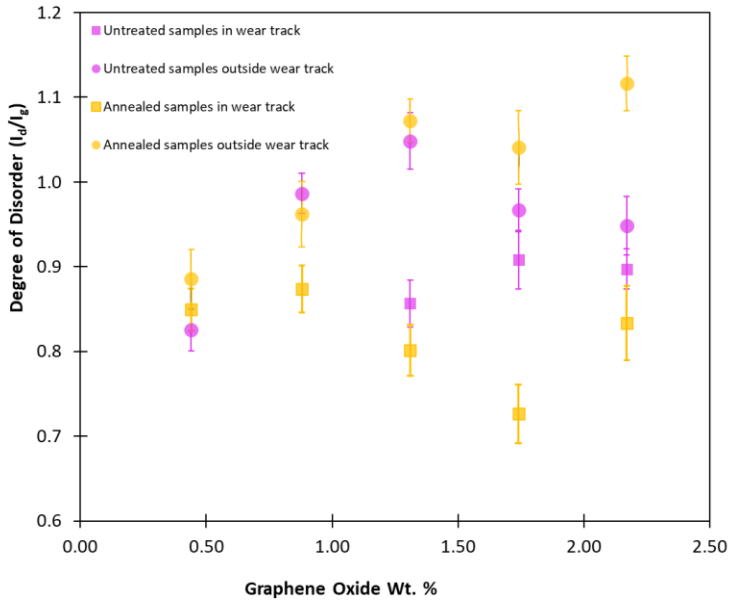

Figure 4.9. Degree of Disorder Id/Ig (extracted from the Micro Raman Spectroscopy of Figure 4.8)

Figure 4.10 shows the pull-off adhesion force measurements from AFM testing on the wear tracks [113], [114]. which generally consists of Van der Waals forces, electrostatic forces, and capillary forces [115]. The results show that most of the samples exhibit higher adhesion force than that of the bare substrate. Only the untreated samples with the least graphene oxide content show an adhesion force less than that of the bare substrate. This is consistent with our understanding that those 2 wear tracks are bare substrate. We note that we would have expected their adhesion force

to be the same as that of the substrate, but we observe a small difference even accounting for the large uncertainty.

A surface exhibiting low adhesion force means that the coating on that surface has been worn by means of a wear mechanism other than adhesion, i.e., abrasive wear as on the titanium substrate. Similarly, the higher the adhesion force exhibited by the surface, the more surface energy it has indicating.

We consider that the friction force (F) (measured during wear tests) is consists of ploughing abrasion and adhesion [104], [116]: $F_{Total}=F_{Adhesion}+F_{Ploughing}$ [117]. In case of alumina sliding against titanium, $F_{Ploughing}$ is much higher than $F_{Adhesion}$, and the total friction is high. For all samples with graphene oxide coating remaining on the worn surface, $F_{Ploughing}$ is at a minimum with a slight increase in $F_{Adhesion}$, so the total friction is reduced.

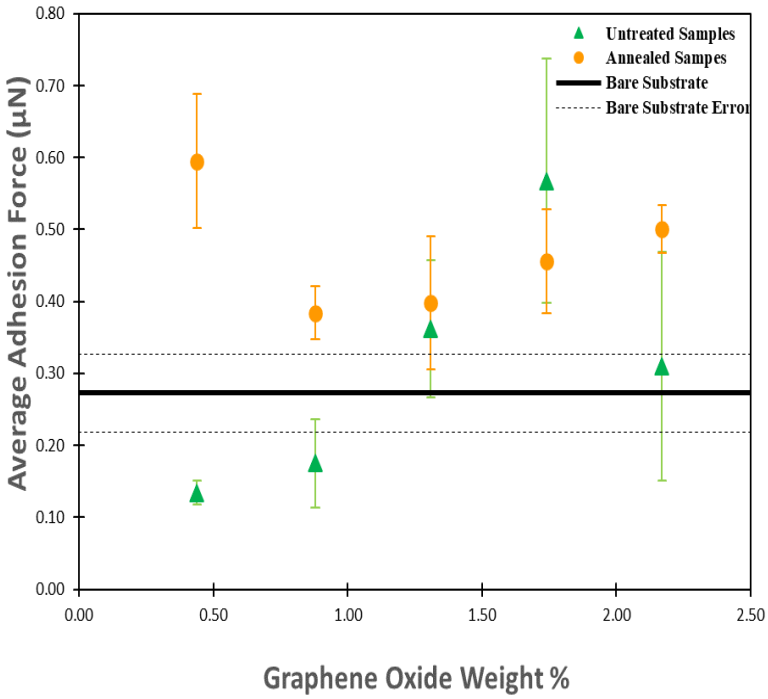

Figure 4.10. Adhesion force measurement obtained by the AFM as function of the graphene oxide content (worn surface)

4.5. Conclusion

This study demonstrates the successful development and evaluation of photocured graphene oxide coatings on titanium substrates. Nematic liquid crystalline structures formed in graphene oxide dispersions in alcohol are used to form the coatings. The estimated degree of nematic ordering in the dispersions increases with increased graphene oxide content to a maximum of ~22%. Photocuring solidifies the coatings, creating covalent bonds between graphene oxide platelets and the substrate, thus enhancing mechanical integrity. The coatings reduce sliding friction compared to bare titanium.

Annealed graphene oxide coatings exhibit consistently low sliding friction coefficient, ~ 0.14, regardless of graphene oxide content. Wear depth analysis indicates that annealing improved coating hardness and adhesion, effectively protecting the substrate. Brittle fracture and fatigue wear are observed in annealed samples, with graphene oxide always present on worn surfaces. A thin, highly bonded layer is crucial for reducing friction and wear. This thin layer likely results from highly ordered platelets near the substrate allowing for strong adhesion and/or tribo-film formation during wear.

Untreated graphene oxide coatings also reduce friction compared to bare titanium but with variable performance depending on graphene oxide content in the dispersion. In the absence of annealing, higher graphene oxide content provides better substrate protection than does lower content. At the lower contents, the graphene oxide coating is completely worn away under a sliding contact, leading to increased friction. Although untreated coatings do not perform as well as annealed ones, they still show notable improvements provided that the graphene oxide content is high enough in the original dispersion.

In summary, photocured graphene oxide coatings on titanium substrates offer a promising approach to enhancing tribological performance. This method provides strong, covalent bonds between graphene oxide layers and the substrate, resulting in durable, low-friction coatings that significantly reduce wear.

Chapter 5. Conclusion and Future Work

5.1. Conclusion

This thesis has explored the development and application of advanced coating technologies, focusing on graphene oxide coatings. Our study has demonstrated that graphene oxide coatings offer significant improvements in mechanical properties, wear resistance, and friction reduction compared to traditional coating materials. The optimization of photocuring parameters has proven essential in enhancing the adhesion and durability of these coatings. By fine-tuning these parameters, we have achieved coatings that meet stringent performance criteria in high-stress environments.

The research presented has also highlighted the critical role of graphene oxide platelet size and distribution in determining the effectiveness of the coatings. Our findings suggest that precise control over these factors can lead to substantial improvements in the wear resistance and overall longevity of the coatings. Furthermore, the investigation into hybrid coatings incorporating other nanomaterials has opened new avenues for enhancing the performance of graphene oxide coatings, particularly in challenging operational conditions.

The results of our study underscore the potential of graphene oxide coatings to revolutionize surface protection in various industrial applications. The improved mechanical properties and enhanced performance characteristics make these coatings suitable for demanding environments, including aerospace and automotive industries.

5.2. Future Work

Building on the findings of this research, several areas warrant further exploration to advance the field of advanced coating technologies:

1. Optimization of Photocuring Parameters:

Future research should focus on refining the photocuring process to further enhance the mechanical properties and adhesion of graphene oxide coatings. Investigating the effects of different curing conditions and additives could lead to more robust and durable coatings.

2. Exploration of Graphene Oxide Platelet Sizes and Distributions:

A deeper examination of how varying platelet sizes and distributions affect the performance of graphene oxide coatings could provide valuable insights for optimizing their properties. This includes studying the impact on wear resistance and friction reduction in different operational contexts.

3. Development of Hybrid Coatings:

The potential benefits of combining graphene oxide with other nanomaterials warrant further investigation. Developing hybrid coatings that leverage the strengths of multiple nanomaterials could yield coatings with superior wear resistance and frictional properties.

4. Long-Term Durability Studies:

To validate the laboratory findings, it is crucial to conduct long-term durability studies in real-world industrial applications. Testing the coatings under operational conditions, such as in aerospace engines, will provide insights into their performance and longevity in practical settings.

5. Scalable Manufacturing Processes:

For widespread adoption of graphene oxide coatings in industrial applications, scalable and cost-effective manufacturing processes need to be developed. Research should focus on optimizing these processes to ensure that the coatings can be produced efficiently without compromising their performance.

Thus, future research can significantly advance the field of advanced coating technologies, enhancing their sustainability and operational efficiency in high-stress environments.

References

[1] K. Holmberg and A. Erdemir, "Influence of tribology on global energy consumption, costs and emissions," *Friction*, vol. 5, no. 3, pp. 263–284, Sep. 2017, doi: 10.1007/s40544-017-0183-5.

[2] B. Swain *et al.*, "Wear: A Serious Problem in Industry," in *Tribology in Materials and Manufacturing - Wear, Friction and Lubrication*, IntechOpen, 2020. doi: 10.5772/intechopen.94211.

[3] "ASME International Mechanical Engineering Congress and Exposition - All Volumes." Accessed: Aug. 01, 2024. [Online]. Available: https://asmedigitalcollection.asme.org/IMECE/volumes/browse-by-conference/IMECE2002/915

[4] C. Shi *et al.*, "Highly-durable hydrophobic and adhesive coatings fabricated from graphene-grafted methacrylate copolymers," *Journal of Applied Polymer Science*, vol. 139, no. 38, p. e52917, 2022, doi: 10.1002/app.52917.

[5] A. R. Marlinda *et al.*, "Graphene as a Lubricant Additive for Reducing Friction and Wear in Its Liquid-Based Form," *Lubricants*, vol. 11, no. 1, Art. no. 1, Jan. 2023, doi: 10.3390/lubricants11010029.

[6] A. B. Scranton, C. N. Bowman, R. W. Peiffer, American Chemical Society, and American Chemical Society, Eds., *Photopolymerization: fundamentals and applications*. in ACS symposium series, no. 673. Washington, DC: American Chemical Society, 1997.

[7] W. A. Braunecker and K. Matyjaszewski, "Controlled/living radical polymerization: Features, developments, and perspectives," *Progress in Polymer Science*, vol. 32, no. 1, pp. 93–146, Jan. 2007, doi: 10.1016/j.progpolymsci.2006.11.002.

[8] M. Schmitt, "Synthesis and testing of ZnO nanoparticles for photo-initiation: experimental observation of two different non-migration initiators for bulk polymerization," *Nanoscale*, vol. 7, no. 21, pp. 9532–9544, May 2015, doi: 10.1039/C5NR00850F.

[9] J. A. Norris, K. Stabile, and R. Jinnah, "An introduction to tribology.," *Journal of surgical orthopaedic advances*, 2008, Accessed: Aug. 02, 2024. [Online]. Available: https://www.semanticscholar.org/paper/An-introduction-to-tribology.-Norris-Stabile/9f133ff7304b8afe0055540b18d8ec0fdb9bf81f

[10] Y. Meng, J. Xu, Z. Jin, B. Prakash, and Y. Hu, "A review of recent advances in tribology," *Friction*, vol. 8, no. 2, pp. 221–300, Apr. 2020, doi: 10.1007/s40544-020-0367-2.

[11] H. Czichos, "Current aspects of tribology," *Wear*, vol. 77, no. 1, pp. 1–11, Mar. 1982, doi: 10.1016/0043-1648(82)90040-0.

[12] A. A. Voevodin, S. D. Walck, and J. S. Zabinski, "Architecture of multilayer nanocomposite coatings with super-hard diamond-like carbon layers for wear protection at high contact loads," *Wear*, vol. 203–204, pp. 516–527, Mar. 1997, doi: 10.1016/S0043-1648(96)07425-X.

[13] A. A. Gharam, M. J. Lukitsch, M. P. Balogh, and A. T. Alpas, "High temperature tribological behaviour of carbon based (B4C and DLC) coatings in sliding contact with aluminum," *Thin Solid Films*, vol. 519, no. 5, pp. 1611–1617, Dec. 2010, doi: 10.1016/j.tsf.2010.07.074.

[14] A. Nidzgorska, M. Witoś, J. Perczyński, and A. Kułaszka, "Aero-engine as the object of tribological research," *Journal of Konbin*, vol. 53, no. 3, pp. 87–128, Sep. 2023, doi: 10.5604/01.3001.0053.9061.

[15] J. A. Dominy, “Tribological design - The aerospace industry,” in *Tribology Series*, vol. 14, D. Dowson, Cm. Taylor, M. Godet, and D. Berthe, Eds., in Tribological Design of Machine Elements, vol. 14. , Elsevier, 1989, pp. 15–21. doi: 10.1016/S0167-8922(08)70176-7.
[16] J. R. Laguna-Camacho *et al.*, “A study of the wear damage on gas turbine blades,” *Engineering Failure Analysis*, vol. 61, Oct. 2015, doi: 10.1016/j.engfailanal.2015.10.002.
[17] M. Ye, X. Yan, and K. He, “Effect of wear damage on aero-thermal performance of the film-cooled squealer tip in a turbine stage,” *Proceedings of the Institution of Mechanical Engineers, Part A: Journal of Power and Energy*, vol. 237, no. 7, pp. 1387–1409, Nov. 2023, doi: 10.1177/09576509231171424.
[18] B. Q. Wang, G. Q. Geng, A. V. Levy, and W. Mack, “Erosivity of particles in circulating fluidized bed combustors,” *Wear*, vol. 152, no. 2, pp. 201–222, Jan. 1992, doi: 10.1016/0043-1648(92)90121-N.
[19] M. Murugan, A. Ghoshal, B. D. Barnett, M. Pepi, K. A. Kerner, and D. T. Booth, “Blade Surface-Particle Interaction and Multifunctional Coatings For Gas Turbine Engine,” in *51st AIAA/SAE/ASEE Joint Propulsion Conference*, in AIAA Propulsion and Energy Forum. , American Institute of Aeronautics and Astronautics, 2015. doi: 10.2514/6.2015-4193.
[20] M. Murugan, A. Ghoshal, M. J. Walock, B. B. Barnett, M. S. Pepi, and K. A. Kerner, “Sand particle-Induced deterioration of thermal barrier coatings on gas turbine blades,” *Advances in aircraft and spacecraft science*, vol. 4, no. 1, pp. 37–52, 2017, doi: 10.12989/aas.2017.4.1.037.
[21] I. Le May, “Case Studies of three fatigue failure evaluations in aircraft,” *Procedia Engineering*, vol. 2, no. 1, pp. 59–64, Apr. 2010, doi: 10.1016/j.proeng.2010.03.006.
[22] R. E. Dundas, “Investigation of Failures in Gas Turbines: Part 1 — Techniques and Principles of Failure Investigation,” doi: 10.1115/93-GT-083.
[23] H. P. Jost, “Paper 26: The Planning and Organization of Lubrication for a New Integrated Iron and Steel Works,” *Proceedings of the Institution of Mechanical Engineers, Conference Proceedings*, vol. 179, no. 4, pp. 287–310, Jun. 1964, doi: 10.1243/PIME_CONF_1964_179_090_02.
[24] “Interview with Luminary Professor H. Peter Jost - The Man who Gave Birth to the Word ‘Tribology.’” Accessed: Mar. 10, 2024. [Online]. Available: https://www.machinerylubrication.com/Read/834/tribology-jost
[25] L. Pejryd, J. Wigren, D. J. Greving, J. R. Shadley, and E. F. Rybicki, “Residual stresses as a factor in the selection of tungsten carbide coatings for a jet engine application,” *JTST*, vol. 4, no. 3, pp. 268–274, Sep. 1995, doi: 10.1007/BF02646970.
[26] P. Behera, R. R. Chromik, and S. Yue, “Effect of Al and Cd sacrificial coatings on the wear of steel substrates,” *Wear*, vol. 477, p. 203847, Jul. 2021, doi: 10.1016/j.wear.2021.203847.
[27] L. Reinert, M. Varenberg, F. Mücklich, and S. Suárez, “Dry friction and wear of self-lubricating carbon-nanotube-containing surfaces,” *Wear*, vol. 406–407, pp. 33–42, Jul. 2018, doi: 10.1016/j.wear.2018.03.021.
[28] B. R. Marple and J. Voyer, “Improved Wear Performance by the Incorporation of Solid Lubricants during Thermal Spraying,” *Journal of Thermal Spray Technology*, vol. 10, no. 4, pp. 626–636, Dec. 2001, doi: 10.1361/105996301770349150.
[29] I. M. Allam, “Solid lubricants for applications at elevated temperatures,” *J Mater Sci*, vol. 26, no. 15, pp. 3977–3984, Aug. 1991, doi: 10.1007/BF02402936.
[30] J. Xu, M. H. Zhu, Z. R. Zhou, P. Kapsa, and L. Vincent, “An investigation on fretting wear life of bonded MoS2 solid lubricant coatings in complex conditions,” *Wear*, vol. 255, no. 1, pp. 253–258, Aug. 2003, doi: 10.1016/S0043-1648(03)00053-X.

[31] H. H. Masjuki *et al.*, “Engine Tribology: Enhancing Energy Efficiency for Cleaner Environment,” in *Diamond-Like Carbon Coatings*, CRC Press, 2022.
[32] M. Hina *et al.*, “Extra Ordinary Properties of Graphene,” in *Graphene: Fabrication, Properties and Applications*, R. T. Subramaniam, R. Kasi, S. Bashir, and S. S. A. Kumar, Eds., Singapore: Springer Nature, 2023, pp. 21–52. doi: 10.1007/978-981-99-1206-3_3.
[33] S. Liu, T. Szkopek, F. Barthelat, and M. Cerruti, “Layered Assembly of Graphene Oxide Paper for Mechanical Structures,” *Langmuir*, vol. 38, no. 29, pp. 8757–8765, Jul. 2022, doi: 10.1021/acs.langmuir.2c00442.
[34] C. M. Almeida *et al.*, “Giant and Tunable Anisotropy of Nanoscale Friction in Graphene,” *Sci Rep*, vol. 6, no. 1, p. 31569, Aug. 2016, doi: 10.1038/srep31569.
[35] W. Liu *et al.*, “Effect of graphene on the microstructure and corrosion resistance of PEO coating formed on D16T aluminum alloy,” *International Journal of Applied Ceramic Technology*, vol. 19, no. 5, pp. 2583–2597, 2022, doi: 10.1111/ijac.14108.
[36] J. Zhang *et al.*, “Graphene-reinforced epoxy powder coating to achieve high performance wear and corrosion resistance,” *Journal of Materials Research and Technology*, vol. 20, pp. 4148–4160, Sep. 2022, doi: 10.1016/j.jmrt.2022.08.156.
[37] D. Özkan, Y. Erarslan, C. Kıncal, O. Gürlü, and M. B. Yağcı, “Wear and corrosion resistance enhancement of chromium surfaces through graphene oxide coating,” *Surface and Coatings Technology*, vol. 391, p. 125595, Jun. 2020, doi: 10.1016/j.surfcoat.2020.125595.
[38] W.-L. Chen, D.-M. Wu, Y. Chen, and Y. Tzeng, “Characterization of Electronic, Electrical, Optical, and Mechanical Properties of Graphene,” in *Nanopackaging: Nanotechnologies and Electronics Packaging*, J. E. Morris, Ed., Cham: Springer International Publishing, 2018, pp. 805–822. doi: 10.1007/978-3-319-90362-0_26.
[39] N. H. Othman, M. Che Ismail, M. Mustapha, N. Sallih, K. E. Kee, and R. Ahmad Jaal, “Graphene-based polymer nanocomposites as barrier coatings for corrosion protection,” *Progress in Organic Coatings*, vol. 135, pp. 82–99, Oct. 2019, doi: 10.1016/j.porgcoat.2019.05.030.
[40] R. Zhang, X. Yu, Q. Yang, G. Cui, and Z. Li, “The role of graphene in anti-corrosion coatings: A review,” *Construction and Building Materials*, vol. 294, p. 123613, Aug. 2021, doi: 10.1016/j.conbuildmat.2021.123613.
[41] Z. Nooralian, M. P. Gashti, and I. Ebrahimi, “Fabrication of a multifunctional graphene/polyvinylphosphonic acid/cotton nanocomposite via facile spray layer-by-layer assembly,” *RSC Adv.*, vol. 6, no. 28, pp. 23288–23299, Feb. 2016, doi: 10.1039/C6RA00296J.
[42] Y. Liu, Z. Dang, Y. Wang, J. Huang, and H. Li, “Hydroxyapatite/graphene-nanosheet composite coatings deposited by vacuum cold spraying for biomedical applications: Inherited nanostructures and enhanced properties,” *Carbon*, vol. 67, pp. 250–259, Feb. 2014, doi: 10.1016/j.carbon.2013.09.088.
[43] M. H. Hassan *et al.*, “Electrically Conductive, Monolithic Metal–Organic Framework–Graphene (MOF@G) Composite Coatings,” *ACS Appl. Mater. Interfaces*, vol. 11, no. 6, pp. 6442–6447, Feb. 2019, doi: 10.1021/acsami.8b20951.
[44] R. Verdejo, M. M. Bernal, L. J. Romasanta, and M. A. Lopez-Manchado, “Graphene filled polymer nanocomposites,” *J. Mater. Chem.*, vol. 21, no. 10, pp. 3301–3310, Feb. 2011, doi: 10.1039/C0JM02708A.
[45] X. Huang, X. Qi, F. Boey, and H. Zhang, “Graphene-based composites,” *Chem. Soc. Rev.*, vol. 41, no. 2, pp. 666–686, Jan. 2012, doi: 10.1039/C1CS15078B.

[46] R. J. Young, I. A. Kinloch, L. Gong, and K. S. Novoselov, “The mechanics of graphene nanocomposites: A review,” *Composites Science and Technology*, vol. 72, no. 12, pp. 1459–1476, Jul. 2012, doi: 10.1016/j.compscitech.2012.05.005.
[47] J. Du and H.-M. Cheng, “The Fabrication, Properties, and Uses of Graphene/Polymer Composites,” *Macromolecular Chemistry and Physics*, vol. 213, no. 10–11, pp. 1060–1077, 2012, doi: 10.1002/macp.201200029.
[48] M. R. Sheikhi, H. Aygun, and O. Altuntas, “Aeroengines: Principles, Components, and Eco-friendly Trends,” in *Materials, Structures and Manufacturing for Aircraft*, M. C. Kuşhan, S. Gürgen, and M. A. Sofuoğlu, Eds., in Sustainable Aviation. , Cham: Springer International Publishing, 2022, pp. 127–151. doi: 10.1007/978-3-030-91873-6_6.
[49] “CO2 emissions from commercial aviation: 2013, 2018, and 2019,” International Council on Clean Transportation. Accessed: Mar. 09, 2024. [Online]. Available: https://theicct.org/publication/co2-emissions-from-commercial-aviation-2013-2018-and-2019/
[50] M. Yilanli, M. R. Sheikhi, O. Altuntas, and E. Açıkkalp, “Assessing the global warming potential of aircraft gas turbine materials: Impacts and implications,” *Process Safety and Environmental Protection*, vol. 175, pp. 764–773, Jul. 2023, doi: 10.1016/j.psep.2023.05.100.
[51] J. Grady *et al.*, “Materials and Processes for New Propulsion Systems with Reduced Environmental Impact,” 2019.
[52] F. Sousa-Cardoso *et al.*, “Graphene-Based Coating to Mitigate Biofilm Development in Marine Environments,” *Nanomaterials*, vol. 13, no. 3, Art. no. 3, Jan. 2023, doi: 10.3390/nano13030381.
[53] T. N. Trung, “Improvement of Environmentally-Friendly Alkyd Composite Coating with Graphene Oxide,” *Malaysian Journal on Composites Science and Manufacturing*, vol. 7, no. 1, Art. no. 1, Mar. 2022, doi: 10.37934/mjcsm.7.1.110.
[54] S. Yang, S. Zhu, and R. Hong, “Graphene Oxide/Polyaniline Nanocomposites Used in Anticorrosive Coatings for Environmental Protection,” *Coatings*, vol. 10, no. 12, Art. no. 12, Dec. 2020, doi: 10.3390/coatings10121215.
[55] S. Chen, H. Hong, and B. Shen, “Substrate-dependent enhancement of the durability of EPD graphene coating as a macroscale solid lubricant,” *Surface and Interface Analysis*, vol. 54, no. 9, pp. 978–985, 2022, doi: 10.1002/sia.7123.
[56] R. Shah, M. Woydt, N. Huq, and A. Rosenkranz, “Tribology meets sustainability,” *Industrial Lubrication and Tribology*, vol. 73, no. 3, pp. 430–435, Jan. 2020, doi: 10.1108/ILT-09-2020-0356.
[57] “Introduction to Liquid Crystals,” in *Liquid Crystals*, John Wiley & Sons, Ltd, 2022, pp. 1–28. doi: 10.1002/9781119705819.ch1.
[58] A. C. Lin *et al.*, “Photonic liquid crystals of graphene oxide for fast membrane nanofiltration,” *Carbon Trends*, vol. 7, p. 100150, Apr. 2022, doi: 10.1016/j.cartre.2022.100150.
[59] R. Carlisle Chambers, E. J. Bell, T. M. Records, A. Cherian, K. Ragan, and B. Swartout, “Cholesteric liquid crystal displays as optical sensors of barbiturate binding,” *Liquid Crystals*, vol. 34, no. 10, pp. 1221–1226, Oct. 2007, doi: 10.1080/02678290701658258.
[60] P. K. Choudhury, A.-B. M. A. Ibrahim, P. K. Choudhury, and A.-B. M. A. Ibrahim, *Liquid Crystals*. 2022. doi: 10.5772/intechopen.95648.
[61] W. A. Braunecker and K. Matyjaszewski, “Controlled/living radical polymerization: Features, developments, and perspectives,” *Progress in Polymer Science*, vol. 32, no. 1, pp. 93–146, Jan. 2007, doi: 10.1016/j.progpolymsci.2006.11.002.

[62] A. Gandini, “Recent Advances In Cationic Polymerization,” in *Integration of Fundamental Polymer Science and Technology—2*, P. J. Lemstra and L. A. Kleintjens, Eds., Dordrecht: Springer Netherlands, 1988, pp. 42–53. doi: 10.1007/978-94-009-1361-5_5.
[63] J. Guan-tai, “Anionic Polymerization in Recent 20 Years,” *Chinese Polymer Bulletin*, 2008, Accessed: Aug. 02, 2024. [Online]. Available: https://www.semanticscholar.org/paper/Anionic-Polymerization-in-Recent-20-Years-Guan-tai/f242cbb1a02b5e03ac3221ac1cd8c51feab5015e
[64] M. Tanabe *et al.*, “Photocontrolled living polymerizations,” *Nature Mater*, vol. 5, no. 6, pp. 467–470, Jun. 2006, doi: 10.1038/nmat1649.
[65] G. R. Davies *et al.*, “Synthesis and properties of stereoregular fluoro-polymers via ring-opening metathesis polymerization of fluorinated norbornenes and norbornadienes. An overview and progress report,” *Makromolekulare Chemie. Macromolecular Symposia*, vol. 66, no. 1, pp. 289–296, 1993, doi: 10.1002/masy.19930660125.
[66] L. Verheyen, P. Leysen, M.-P. Van Den Eede, W. Ceunen, T. Hardeman, and G. Koeckelberghs, “Advances in the controlled polymerization of conjugated polymers,” *Polymer*, vol. 108, pp. 521–546, Jan. 2017, doi: 10.1016/j.polymer.2016.09.085.
[67] D. Morselli, F. Bondioli, M. Sangermano, and M. Messori, “Photo-cured epoxy networks reinforced with TiO2 in-situ generated by means of non-hydrolytic sol-gel process,” *Polymer*, vol. 53, pp. 283–290, Jan. 2012, doi: 10.1016/j.polymer.2011.12.006.
[68] “Wear: A Serious Problem in Industry,” Dec. 2020, doi: 10.5772/INTECHOPEN.94211.
[69] K. Holmberg and A. Erdemir, “Influence of tribology on global energy consumption, costs and emissions,” *Friction*, vol. 5, no. 3, pp. 263–284, Sep. 2017, doi: 10.1007/s40544-017-0183-5.
[70] X. Xie, J. Xu, and J. Luo, “Analysis of skid damage to cylindrical roller bearing of mainshaft of aeroengine,” *J Mech Sci Technol*, vol. 34, no. 8, pp. 3239–3247, Aug. 2020, doi: 10.1007/s12206-020-0716-0.
[71] G. Gautier, M. G. Faga, and V. Tebaldo, “Impact Wear Resistance of Nanocomposite Coatings for Aircraft Components,” *Key Engineering Materials*, vol. 813, pp. 387–392, 2019, doi: 10.4028/www.scientific.net/KEM.813.387.
[72] D. K. Devarajan, B. Rangasamy, and K. K. Amirtharaj Mosas, “State-of-the-Art Developments in Advanced Hard Ceramic Coatings Using PVD Techniques for High-Temperature Tribological Applications,” *Ceramics*, vol. 6, no. 1, Art. no. 1, Mar. 2023, doi: 10.3390/ceramics6010019.
[73] C. Zhang, L. Liu, K. C. Chan, Q. Chen, and C. Y. Tang, “Wear behavior of HVOF-sprayed Fe-based amorphous coatings,” *Intermetallics*, vol. 29, pp. 80–85, Oct. 2012, doi: 10.1016/j.intermet.2012.05.004.
[74] C. Munteanu *et al.*, “Study of the wear behavior of bronze coatings deposited by the EAS method,” *Journal of Engineering Sciences and Innovation*, vol. 7, pp. 415–426, Dec. 2022, doi: 10.56958/jesi.2022.7.4.415.
[75] S. C. Tung and M. L. McMillan, “Automotive tribology overview of current advances and challenges for the future,” *Tribology International*, vol. 37, no. 7, pp. 517–536, Jul. 2004, doi: 10.1016/j.triboint.2004.01.013.
[76] D. Dowson, C. M. Taylor, and M. Godet, *Developments in Numerical and Experimental Methods Applied to Tribology: Proceedings of the 10th Leeds–Lyon Symposium on Tribology Held at the Institut National des Sciences Appliquées, Lyon, France, 6th–9th September 1983*. Elsevier, 2014.

[77] M. B. Beardsley, P. G. Happoldt, K. C. Kelley, E. F. Rejda, and D. F. Socie, "Thermal Barrier Coatings For Low Emission, High Efficiency Diesel Engine Applications," SAE International, Warrendale, PA, SAE Technical Paper 1999-01–2255, Apr. 1999. doi: 10.4271/1999-01-2255.

[78] R. K. Jensen, S. Korcek, and M. D. Johnson, "Friction-reducing and antioxidant capabilities of engine oil additive systems under oxidative conditions. II. Understanding ligand exchange in a molybdenum dialkyldithiocarbamate/zinc dialkyldithiophosphate additive system in various base oils," *Lubrication Science*, vol. 14, no. 1, pp. 25–42, 2001, doi: 10.1002/ls.3010140103.

[79] A. Erdemir, "Review of engineered tribological interfaces for improved boundary lubrication," *Tribology International*, vol. 38, no. 3, pp. 249–256, Mar. 2005, doi: 10.1016/j.triboint.2004.08.008.

[80] A. K. Misra, "Durability Challenges for Next Generation of Gas Turbine Engine Materials," presented at the AVT Symposium on Design, Modelling, Lifting and Validation of Advanced Materials in Extreme Military Environments, Biarritz, Oct. 2012. Accessed: Mar. 09, 2024. [Online]. Available: https://ntrs.nasa.gov/citations/20130010776

[81] R. R. Boyer, J. D. Cotton, M. Mohaghegh, and R. E. Schafrik, "Materials considerations for aerospace applications," *MRS Bulletin*, vol. 40, no. 12, pp. 1055–1066, Dec. 2015, doi: 10.1557/mrs.2015.278.

[82] D. A. Exarchos *et al.*, "Development and characterization of environmentally friendly multifunctional protective coatings," in *NDE 4.0, Predictive Maintenance, and Communication and Energy Systems in a Globally Networked World*, SPIE, Apr. 2022, pp. 102–116. doi: 10.1117/12.2614989.

[83] M. L. Grilli *et al.*, "Critical Raw Materials Saving by Protective Coatings under Extreme Conditions: A Review of Last Trends in Alloys and Coatings for Aerospace Engine Applications," *Materials*, vol. 14, no. 7, Art. no. 7, Jan. 2021, doi: 10.3390/ma14071656.

[84] B. Postolnyi *et al.*, "Multilayer and high-entropy alloy-based protective coatings for solving the issue of critical raw materials in the aerospace industry," *IOP Conf. Ser.: Mater. Sci. Eng.*, vol. 1024, no. 1, p. 012009, Jan. 2021, doi: 10.1088/1757-899X/1024/1/012009.

[85] K. Cui and Y. Zhang, "High-Entropy Alloy Films," *Coatings*, vol. 13, no. 3, Art. no. 3, Mar. 2023, doi: 10.3390/coatings13030635.

[86] C. Lin and Y. Yao, "Corrosion-Resistant Coating Based on High-Entropy Alloys," *Metals*, vol. 13, no. 2, Art. no. 2, Feb. 2023, doi: 10.3390/met13020205.

[87] J. E. Kim *et al.*, "Graphene Oxide Liquid Crystals," *Angewandte Chemie International Edition*, vol. 50, no. 13, pp. 3043–3047, 2011, doi: 10.1002/anie.201004692.

[88] L. K. Shrestha *et al.*, "Nonionic amphiphile nanoarchitectonics: self-assembly into micelles and lyotropic liquid crystals," *Nanotechnology*, vol. 26, no. 20, p. 204002, May 2015, doi: 10.1088/0957-4484/26/20/204002.

[89] Z. Xu and C. Gao, "Aqueous liquid crystals of graphene oxide," *ACS Nano*, vol. 5, no. 4, pp. 2908–2915, Apr. 2011, doi: 10.1021/nn200069w.

[90] S. Naficy *et al.*, "Graphene Oxide Dispersions: Tuning Rheology to Enable Fabrication," *Materials Horizons*, pp. 295–366, Jan. 2014, doi: 10.1039/C3MH00144J.

[91] H. Pan, S. Zhu, and L. Mao, "Graphene Nanoarchitectonics: Approaching the Excellent Properties of Graphene from Microscale to Macroscale," *Journal of Inorganic and Organometallic Polymers and Materials*, vol. 25, Mar. 2014, doi: 10.1007/s10904-014-0073-5.

[92] Y. Zhang *et al.*, “Graphene-based artificial nacre nanocomposites,” *Chem. Soc. Rev.*, vol. 45, no. 9, pp. 2378–2395, May 2016, doi: 10.1039/C5CS00258C.
[93] D. Wu, F. Zhang, H. Liang, and X. Feng, “Nanocomposites and macroscopic materials: assembly of chemically modified graphene sheets,” *Chem. Soc. Rev.*, vol. 41, no. 18, pp. 6160–6177, Aug. 2012, doi: 10.1039/C2CS35179J.
[94] K. B. Riad, S. V. Hoa, and P. M. Wood-Adams, “Photocuring Graphene Oxide Liquid Crystals for High-Strength Structural Materials,” *ACS Omega*, vol. 7, no. 24, pp. 21192–21198, Jun. 2022, doi: 10.1021/acsomega.2c02084.
[95] R. Jalili *et al.*, “Organic Solvent-Based Graphene Oxide Liquid Crystals: A Facile Route toward the Next Generation of Self-Assembled Layer-by-Layer Multifunctional 3D Architectures,” *ACS Nano*, vol. 7, no. 5, pp. 3981–3990, May 2013, doi: 10.1021/nn305906z.
[96] D. Morselli, F. Bondioli, M. Sangermano, and M. Messori, “Photo-cured epoxy networks reinforced with TiO2 in-situ generated by means of non-hydrolytic sol–gel process,” *Polymer*, vol. 53, no. 2, pp. 283–290, Jan. 2012, doi: 10.1016/j.polymer.2011.12.006.
[97] J. Ellis, S. Allen, Y. Chim, C. Roberts, S. Tendler, and M. Davies, “Molecular-Scale Studies on Biopolymers Using Atomic Force Microscopy,” in *Advances in Polymer Science*, vol. 193, 2005, pp. 123–172. doi: 10.1007/12_027.
[98] J. Y. Oh, J. Park, Y. C. Jeong, J. H. Kim, S. J. Yang, and C. R. Park, “Secondary Interactions of Graphene Oxide on Liquid Crystal Formation and Stability,” *Particle & Particle Systems Characterization*, vol. 34, no. 9, p. 1600383, 2017, doi: 10.1002/ppsc.201600383.
[99] F. Lin, X. Tong, Y. Wang, J. Bao, and Z. M. Wang, “Graphene oxide liquid crystals: synthesis, phase transition, rheological property, and applications in optoelectronics and display,” *Nanoscale Res Lett*, vol. 10, no. 1, p. 435, Nov. 2015, doi: 10.1186/s11671-015-1139-1.
[100] B. Szewczyková, P. Blaškovitš, E. Hodúlová, and E. Lechovi, “STUDY AND CHARACTERISTIC OF ABRASIVE WEAR MECHANISMS,” 2009. Accessed: Apr. 17, 2024. [Online]. Available: https://www.semanticscholar.org/paper/STUDY-AND-CHARACTERISTIC-OF-ABRASIVE-WEAR-Szewczykov%C3%A1-Bla%C5%A1kovit%C5%A1/35d05689f176bb64e7e69713519912025a2bce12
[101] G. W. Stachowiak and A. W. Batchelor, Eds., “14 Fatigue Wear,” in *Tribology Series*, vol. 24, in Engineering TriBology, vol. 24. , Elsevier, 1993, pp. 657–681. doi: 10.1016/S0167-8922(08)70588-1.
[102] J. D. Gates, “Two-body and three-body abrasion: A critical discussion,” *Wear*, vol. 214, no. 1, pp. 139–146, Jan. 1998, doi: 10.1016/S0043-1648(97)00188-9.
[103] S. Glodež, Z. Ren, and J. Flašker, “Surface fatigue of gear teeth flanks,” *Computers & Structures*, vol. 73, no. 1, pp. 475–483, Oct. 1999, doi: 10.1016/S0045-7949(98)00251-X.
[104] K. Holmberg, H. Ronkainen, A. Laukkanen, and K. Wallin, “Friction and wear of coated surfaces — scales, modelling and simulation of tribomechanisms,” *Surface and Coatings Technology*, vol. 202, pp. 1034–1049, Dec. 2007, doi: 10.1016/j.surfcoat.2007.07.105.
[105] F. T. Johra, J.-W. Lee, and W.-G. Jung, “Facile and safe graphene preparation on solution based platform,” *Journal of Industrial and Engineering Chemistry*, vol. 20, no. 5, pp. 2883–2887, Sep. 2014, doi: 10.1016/j.jiec.2013.11.022.
[106] D. L. Matz, H. Sojoudi, S. Graham, and J. E. Pemberton, “Signature Vibrational Bands for Defects in CVD Single-Layer Graphene by Surface-Enhanced Raman Spectroscopy,” *J. Phys. Chem. Lett.*, vol. 6, no. 6, pp. 964–969, Mar. 2015, doi: 10.1021/jz5027272.

[107] S.-R. Cho and H.-G. Cho, “Characterization of Black Carbon Collected from Candle Light and Automobile Exhaust Pipe,” *Journal of the Korean Chemical Society*, vol. 57, no. 6, pp. 691–696, 2013, doi: 10.5012/jkcs.2013.57.6.691.
[108] A. Lee *et al.*, “Raman study of D* band in graphene oxide and its correlation with reduction,” *Applied Surface Science*, vol. 536, p. 147990, Jan. 2021, doi: 10.1016/j.apsusc.2020.147990.
[109] M. Yoshikawa, M. Murakami, and Y. Fujita, “Characterization of inhomogeneity at edges of graphene oxide films using tip-enhanced Raman spectroscopy,” *Journal of Raman Spectroscopy*, vol. 53, no. 8, pp. 1394–1401, 2022, doi: 10.1002/jrs.6374.
[110] D. López Díaz, M. Holgado, J. Fierro, and M. M. Velázquez, “The Evolution of the Raman Spectrum With the Chemical Composition of Graphene Oxide,” *The Journal of Physical Chemistry C*, vol. 121, Aug. 2017, doi: 10.1021/acs.jpcc.7b06236.
[111] Z. Yang, Y. Sun, and F. Ma, “Interlayer spacing of multilayer graphene oxide: Influences of oxygen-containing group density, thickness, temperature and strain,” *Applied Surface Science*, vol. 529, p. 147075, Nov. 2020, doi: 10.1016/j.apsusc.2020.147075.
[112] P. Gavallas, D. Savvas, and G. Stefanou, “Mechanical properties of graphene nanoplatelets containing random structural defects,” *Mechanics of Materials*, vol. 180, p. 104611, May 2023, doi: 10.1016/j.mechmat.2023.104611.
[113] M. Pierce, J. Stuart, A. Pungor, P. Dryden, and V. Hlady, “Adhesion Force Measurements Using an Atomic Force Microscope Upgraded with a Linear Position Sensitive Detector,” *Langmuir*, vol. 10, no. 9, pp. 3217–3221, Sep. 1994, doi: 10.1021/la00021a053.
[114] O. Marti, “Measurement of Adhesion and Pull-Off Forces with the AFM,” in *Modern Tribology Handbook: Volume One: Principles of Tribology*, 2000. doi: 10.1201/9780849377877.ch17.
[115] T. Jiang and Y. Zhu, “Measuring graphene adhesion using atomic force microscopy with a microsphere tip,” *Nanoscale*, vol. 7, no. 24, pp. 10760–10766, Jun. 2015, doi: 10.1039/C5NR02480C.
[116] the late F. P. Bowden and D. Tabor, *The Friction and Lubrication of Solids*. in Oxford Classic Texts in the Physical Sciences. Oxford, New York: Oxford University Press, 2001.
[117] S. Lafaye, “True solution of the ploughing friction coefficient with elastic recovery in the case of a conical tip with a blunted spherical extremity,” *Wear*, vol. 264, no. 7, pp. 550–554, Mar. 2008, doi: 10.1016/j.wear.2007.04.005.

Appendix

Supporting Information for:

Photocured graphene-oxide liquid crystal coatings for improved tribological performance

Mina. E. Farid [a], *Paula M. Wood-Adams* [b*], *Pantcho P. Stoyanov* [c]

[a] Department of Mechanical, Industrial and Aerospace Engineering, Concordia University, Montreal, QC H3G 1M8, Canada

[b] Department of Engineering, University of Northern British Columbia, Prince George, BC V2N 4Z9, Canada

[c] Department of Chemical and Materials Engineering, Concordia University, Montreal, QC H3G 1M8, Canada

[*] **Corresponding Author**

Email: paula.wood-adams@unbc.ca

Figure S1 shows photocured samples.

Figure S1. Specimens with photocured coating with the upper row annealed at 190 °C for 2 hours (marked A), and others left untreated. The bare titanium substrate is on the left. The weights of graphene oxide used in the dispersions are shown below each sample.

Figure S2 shows the annealed sample with the highest graphene oxide content (2.17 wt.%) exhibiting swelling in the coating film due to the vaporization of trapped molecules, leading to increased porosity [1], [2].

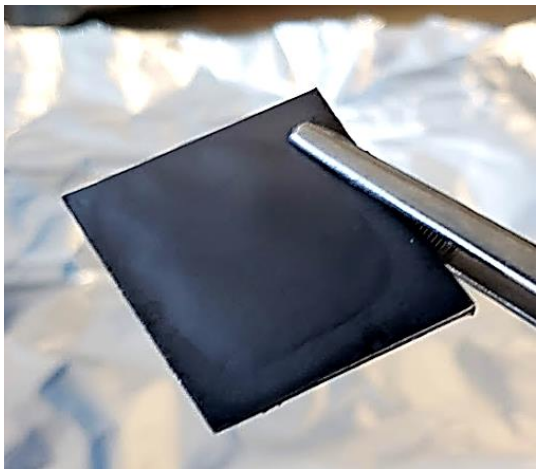

Figure S2. Annealed sample of 2.17 Wt. % Graphene Oxide exhibiting coating swelling

Figure S3 shows the average friction coefficient for each graphene oxide concentration over 5000 wear cycles. The untreated sample with 1.31 wt.% graphene oxide exhibits mixed results, with one set showing no friction reduction after 2500 cycles and another showing a low friction coefficient, indicating transitional behavior.

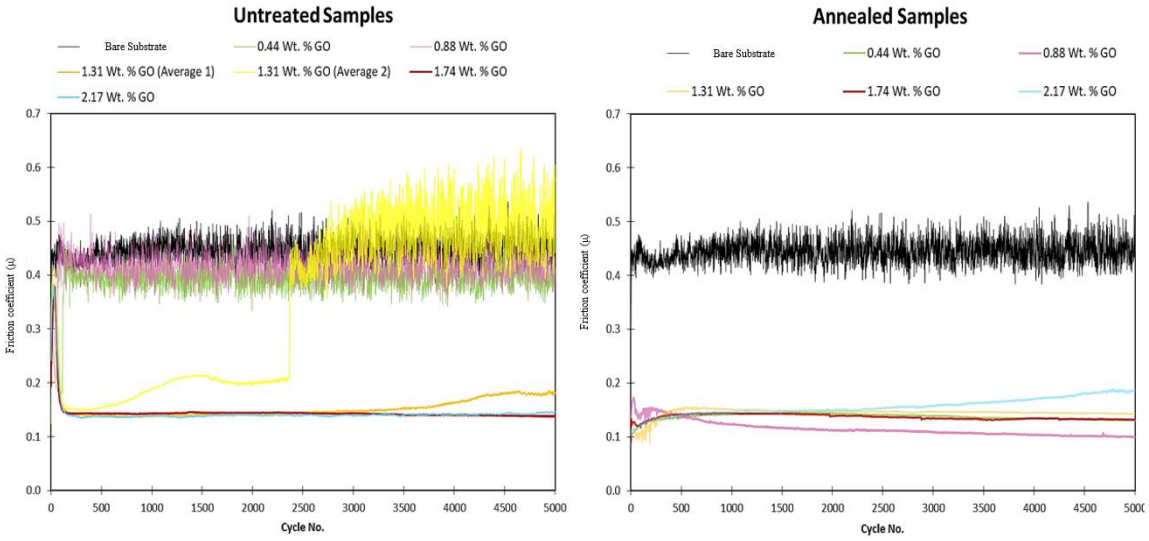

Figure S3. Average friction coefficient as function of the number of cycles (sliding wear test)

Figure S4 shows the average wear profiles of all samples collected using confocal microscopy from multiple cross sections of the wear tracks.

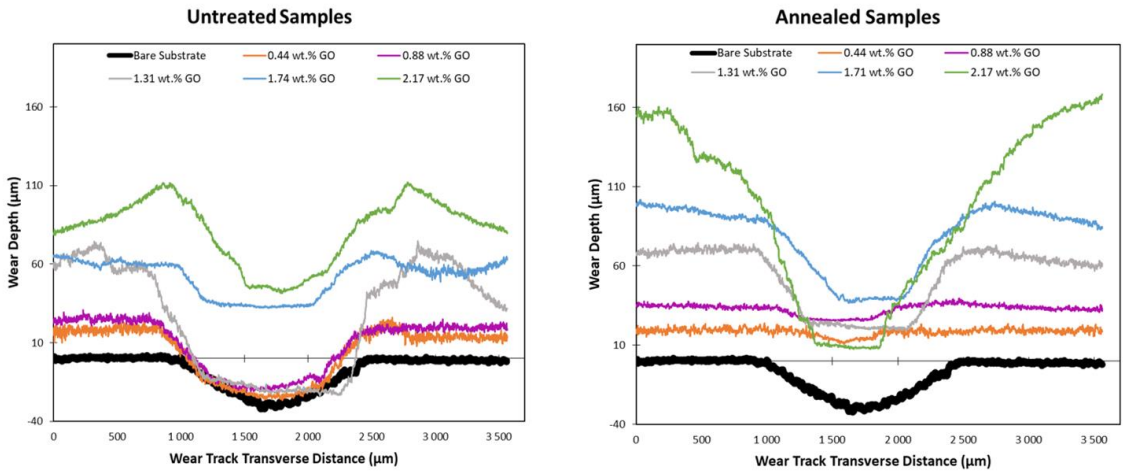

Figure S4. Average wear profiles plotted for all samples

Figures 3A, 5, and S3 show that the untreated coating with 1.31 wt.% graphene oxide exhibits transitional behavior. Figure S5 displays the alumina counter faces after the sliding wear tests for the 1.31 wt.% untreated sample. Figure S5A shows a counter face having experienced contact with the substrate. In contrast, Figure S5B suggests that the graphene layer remained intact, preventing substrate contact.

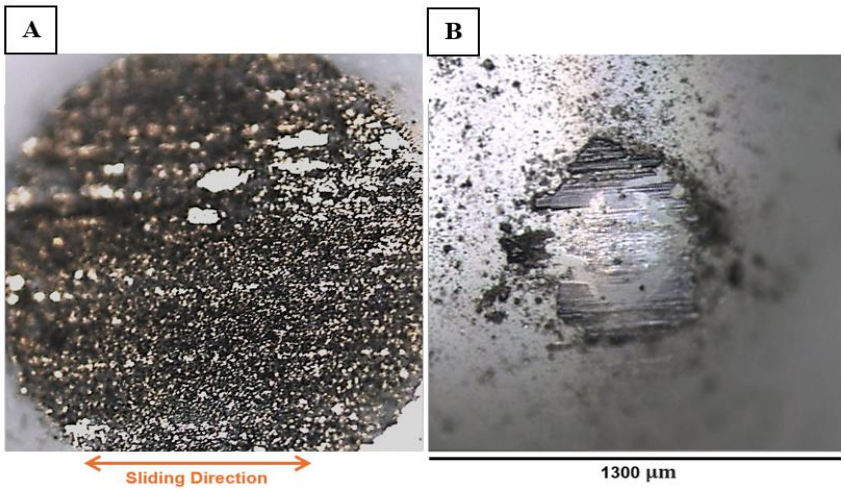

Figure S5. Worn alumina counter faces from sliding wear tests for 2 different locations on the specimen of the 1.31 wt.% graphene oxide, untreated sample.

Figure S6 presents the elemental analysis of the wear track for the sample containing 0.44 wt.% graphene oxide. The darker areas, corresponding to spectra 1 and 3, show a high concentration of graphene oxide, as indicated by the significant presence of carbon. While spectra 2 and 4, representing the grey areas, show a lower concentration of graphene oxide, its presence is confirmed by the micro-Raman analysis shown in Figure 8.

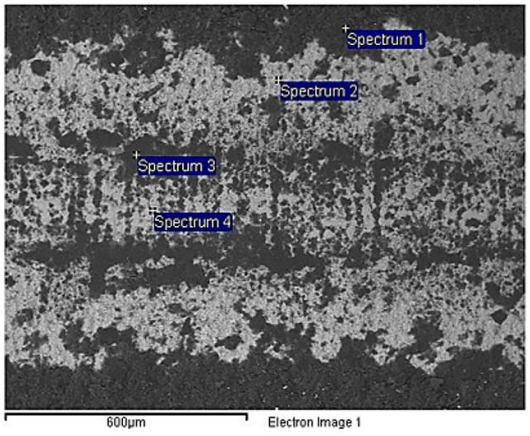

Spectrum	In stats.	C	O	Al	P	Ti	Total
Spectrum 1	Yes	81.18	13.26	0.00	5.56	0.00	100
Spectrum 2	Yes	3.94	21.25	5.38	0.00	69.43	100
Spectrum 3	Yes	56.84	24.40	1.01	3.55	14.20	100
Spectrum 4	Yes	17.63	27.54	3.69	2.31	48.84	100
Mean		39.90	21.61	2.52	2.85	33.12	100
Std. deviation		35.50	6.13	2.46	2.33	31.73	
Max.		81.18	27.54	5.38	5.56	69.43	
Min.		3.94	13.26	0.00	0.00	0.00	

Figure S6. Elemental analysis of the wear track for the treated sample containing 0.44 wt.% graphene oxide.

A similar observation to that in Figure S6 applies to Figure S7, which presents the elemental analysis of the treated sample containing 0.88 wt.% graphene oxide.

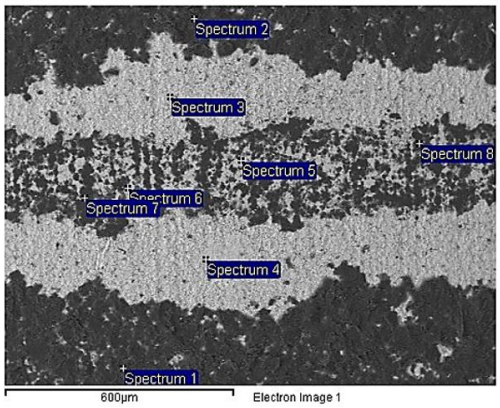

Spectrum	In stats.	C	O	Al	P	Ti	V	Total
Spectrum 1	Yes	82.81	13.88	0.00	1.63	1.68	0.00	100
Spectrum 2	Yes	76.56	14.26	0.00	2.04	7.15	0.00	100
Spectrum 3	Yes	3.28	0.00	5.56	0.00	85.87	5.28	100
Spectrum 4	Yes	0.00	0.00	6.40	0.00	89.92	3.69	100
Spectrum 5	Yes	2.82	0.00	5.54	0.00	88.55	3.09	100
Spectrum 6	Yes	6.36	23.58	4.47	0.84	64.75	0.00	100
Spectrum 7	Yes	62.86	16.10	1.28	1.63	18.13	0.00	100
Spectrum 8	Yes	78.65	14.67	0.00	2.01	4.66	0.00	100
Mean		39.17	10.31	2.91	1.02	45.09	1.51	100
Std. deviation		38.99	9.07	2.84	0.92	40.77	2.17	
Max.		82.81	23.58	6.40	2.04	89.92	5.28	
Min.		0.00	0.00	0.00	0.00	1.68	0.00	

Figure S7. Elemental analysis of the wear track for the treated sample containing 0.88 wt.% graphene oxide.

Refences

[1] Z. Yang, Y. Sun, and F. Ma, “Interlayer spacing of multilayer graphene oxide: Influences of oxygen-containing group density, thickness, temperature and strain,” *Applied Surface Science*, vol. 529, p. 147075, Nov. 2020, doi: 10.1016/j.apsusc.2020.147075.

[2] P. Gavallas, D. Savvas, and G. Stefanou, “Mechanical properties of graphene nanoplatelets containing random structural defects,” *Mechanics of Materials*, vol. 180, p. 104611, May 2023, doi: 10.1016/j.mechmat.2023.104611.